REMARKS

Claims 1, 2, 14, 17-20, 23, 29, and 32-43 are pending in this application. All of the claims were rejected under the judicially created doctrine of obviousness-type double patenting. Claims 1, 2, 14, 17-20, 29, 32-40, and 43-44 were rejected under 35 U.S.C. § 112, first paragraph. Claim 20 was also rejected under 35 U.S.C. § 112, second paragraph. All of the claims were rejected under 35 U.S.C. § 103(a) for obviousness. Each of the Office's rejections is addressed below. Applicants respectfully request reconsideration of the claims as amended.

Support for the amendments

Claim 1 has been amended to delete the term "murine." Support for this amendment may be found, for example, in original claims 1, 5, and 16. Other claim amendments have been made to correct claim dependencies and typographical errors. New dependent claims 44 to 55, directed to combined compositions, have been added. Support for these claims may be found, for example, for example, at page 32, lines 11 to 15. No new matter has been added by these amendments.

Rejections under the Judicially Created Doctrine of Obviousness-Type Double Patenting

Claim 41 was rejected under the judicially created doctrine of obviousness-type double patenting as being unpatentable over claim 9 of U.S. Patent No. 5,747,272.

Claims 1-2, 14, 17-20, 23, 29, and 32-43 were rejected under the judicially created doctrine of obviousness-type double patenting as being unpatentable over claim 9 of U.S. Patent No. 5,747,272 in view of Carter et al. (WO 94/04679; "Carter"). Applicants will address each of these rejections, if appropriate, upon an indication of otherwise allowable subject matter.

Rejections under 35 U.S.C. § 112, first paragraph

Claims 1, 2, 14, 17-20, 29, 32-40, and 43-44 were rejected under 35 U.S.C. § 112, first paragraph. Although acknowledging that applicants' specification enables humanized monoclonal antibodies based on monoclonal antibodies 13C4 or 11E10, the examiner has maintained the rejection on the grounds that:

> [T]he specification is silent on the sequences of the murine variable region required to confer function on the chimeric antibody the location (or sequence) of the immunogenic epitopes. Given the lack of guidance contained in the specification and the unpredictability in determining acceptable sequence variations, one of skill in the art could not make the broadly claimed invention without undue experimentation.

For the following reasons, applicants respectfully disagree.

Contrary to the examiner's assertion, applicants' specification clearly sets forth the sequences of the variable regions as well as specific complementarity determining region (CDR) sequences required to confer binding to Shiga toxin protein. For example, at page 9, lines 18-20, the specification states, "... the CDRs of the variable region are employed in the invention. [These] CDRs are located in the variable regions of both the light and

heavy chains and ***are responsible for antigen binding***" (emphasis added). Both the entire variable region sequences and the individual CDRs for the heavy and light chain are set forth in Figure 3, for the antibodies based on monoclonal antibody 13C4, and Figure 6, for the antibodies based on monoclonal antibody 11E10.

Applicants further note that all of the claimed humanized monoclonal antibodies recite sequences based on the defined regions of monoclonal antibodies 13C4 and 11E10, which the examiner has acknowledged are enabled by applicants' specification. Applicants point out that, having access to applicants' newly disclosed immunoglobulin variable regions and CDR gene sequences based on monoclonal antibodies 13C4 and 11E10, their specification enables the identification of additional nucleic acid molecules encoding an immunoglobulin variable region falling within applicants' claims absent "undue experimentation," simply by following the teachings found in applicants' specification in combination with standard methods known in the art at the time of applicants' invention.

Any "experimentation" involved in isolating and characterizing additional variable regions falling within the present claims is straightforward, and is rendered so by applicants' discovery of the sequences encoding the 13C4 and 11E10 immunoglobulin variable regions. Specifically, if one skilled in the art wished to produce additional variable region sequences, they would simply use, for example, applicants' disclosed variable region sequences as a template in combination with conventional mutagenesis

methodologies, such as alanine scanning, site-directed mutagenesis, or saturation mutagenesis.[1] Monoclonal antibodies having sequences encoding variable regions that include, for example, at least part of an immunoglobulin variable region falling within the scope of the claims are then tested for binding to Shiga toxin protein, for example, Stx1 or Stx2, using the assays outlined in applicants' specification. (See, for example, Example 3 and Example 6.) Accordingly, there is no basis for concluding that one skilled in the art, once equipped with applicants' disclosed sequences, would not be able to isolate a reasonable number of sequences encoding at least part of an immunoglobulin variable region falling within the scope of the present claims.

In addition, the examiner also notes that the features upon which the applicants' rely, for example, that the claimed antibody must bind antigen, are not recited in the claim. Applicants note, however, that the claims are directed to a "humanized monoclonal antibody that binds to Shiga toxin protein" or "humanized monoclonal antibody which binds Shiga toxin type 2 and Shiga toxin type 2 variants." Furthermore, to the extent the examiner requires applicants' claims to include specific epitope sequences, this requirement finds no basis in the law.

Applicants also point out that, to sustain an enablement rejection, the Office has

---

[1] See, for example, Near et al., Characterization of an Anti-Digoxin Antibody Binding Site by Site-Directed Mutagenesis, *Molecular Immunology* 30:369-377, 1993 (copy enclosed); Chatellier et al., Codon-Based Combinatorial Alanine Scanning Site-Directed Mutagenesis: Design, Implementation, and Polymerase Chain Reaction Screening, *Analytical Biochemistry* 229:282-290, 1995 (copy enclosed); and Jeffrey et al., The X-ray Structure of an Anti-Tumour Antibody in Complex with Antigen, *Nature Structural Biology* 2:466-471, 1995 (copy enclosed).

the initial burden to establish a reasonable basis to question the enabling nature of an applicant's specification. Thus, in a case in which the PTO questions the enablement of a claim, the CCPA, in *In re Marzocchi*, 439 F.2d 220, 223, 169 USPQ 367, 369 (CCPA 1971) has stated that:

> a specification disclosure which contains a teaching of the manner and process of making and using the invention in terms which correspond in scope to those used in describing and defining the subject matter sought to be patented must be taken as in compliance with the enabling requirement of the first paragraph of § 112 unless there is reason to doubt the objective truth of the statements contained therein which must be relied on for enabling support (emphasis added).

The MPEP (§ 2164.04) further emphasizes the *Marzocchi* standard in stating that:

> it is incumbent upon the Patent Office, whenever a rejection on this basis is made, to explain why it doubts the truth or accuracy of any statement in a supporting disclosure and to back up assertions of its own with acceptable evidence or reasoning which is inconsistent with the contested statement. Otherwise there would be no need for the applicant to go to the trouble and expense of supporting his presumptively accurate disclosure (emphasis added).

Here, applicants note that no scientific evidence currently made of record in this case establishes a basis for doubting the objective truth of the statements found in applicants' specification regarding enablement with respect to isolating at least a part of an immunoglobulin variable region falling within applicants' claims and determining whether such sequences bind to Shiga toxin protein. Moreover, the examiner has provided no evidence or reason for doubting applicants' statement that other variable regions falling within the scope of the claims would function similarly as those described

for 13C4 and 11E10. On this basis, as well, the facts in the present case compel withdrawal of the § 112, first paragraph enablement rejection, and applicants request reconsideration on this issue.

In also rejecting claims 23, 29, and 39-40, the examiner states:

> Claims 23, 29 and 39-40 are rejected under 35 U.S.C. 112, first paragraph, because the specification, while being enabling for pharmaceutical compositions comprising humanized monoclonal antibodies based on monoclonal antibodies 13C4 or 11E10 (defined sequences), does not reasonable provide enablement for pharmaceutical compositions comprising humanized antibodies "containing at least part of a murine immunoglobulin variable regions as shown in Figure 3 (SEQ ID NO.:21 or Figure 6 (SEQ ID NO.: 42), wherein the antibody specifically reacts with Stx1 or Stx2 antigen or portions of SEQ ID NO.:42 or SEQ ID NO.:44 mainly for the reasons set forth in the previous Office action in the rejection of claims 23 and 29. The specification does not enable any person skilled in the art to which it pertains, or with which it is most nearly connected, to make and/or use the invention commensurate in scope with these claims. Contrary to Applicant's assertion, the amendment to claim 1 is not sufficient to obviate the aforementioned rejection. As outlined previously, the specification is silent on how the claimed compositions would be used and equally silent on the efficacy of a give composition. Since no evidence has been provided that illustrates or even suggests that the claimed pharmaceutical compositions are capable of eliciting a beneficial therapeutic response, one of skill in the are would be able to make and use the claimed invention.

As is discussed above, applicants have addressed the examiner's specific concern regarding the specification's guidance for producing humanized antibodies containing at least part of an immunoglobulin variable region falling within the scope of the claims.

With respect to the examiner's contention that "no evidence has been provided that illustrates or even suggests that the claimed pharmaceutical compositions are capable of

eliciting a beneficial therapeutic response," applicants submit that this basis for the § 112 rejection — while cast in enablement terms — is, in reality, a utility rejection and should be properly evaluated under the Utility Examination Guidelines published in the Federal Register in July 1995 and now cited in the MPEP at § 706.03(a) and §§ 2107-2107.02. These Guidelines and the accompanying Legal Analysis apply to rejections based upon lack of utility, whether cited under 35 U.S.C § 101 or under § 112, first paragraph, as in the present case. The standard is whether the efficacy of a therapeutic is believable to those skilled in the art. Applying this standard to the present case, the § 112 rejection should clearly be withdrawn.

Moreover, as noted in the Guidelines, to uphold this ground for the § 112 rejection, the examiner must establish the present case as one of those rare instances which meets the stringent criteria for rejection described in the Legal Analysis, i.e., "totally incapable of achieving a useful result." Brooktree Corp. v. Advanced Micro Devices, Inc., 977 F.2d 1555, 1571, 24 USPQ2d 1401 (Fed. Cir. 1992), as cited in the Legal Analysis, page 2, lines 44-45. According to the Legal Analysis, the only instances in which the Federal courts have found a lack of patentable utility was where, "based upon the factual record of the case, it was clear that the invention could and did not work as the inventor claimed it did." (Legal Analysis page 3, lines 10-12). These rare cases have been ones in which the applicant either (a) failed to disclose any utility for the invention or (b) asserted a utility that could be true only "if it violated a scientific principle, such as the second law

of thermodynamics, or a law of nature, or was wholly inconsistent with contemporary knowledge in the art." (Legal Analysis page 9, lines 10-16).

Clearly, no such evidence is present in this case, and the use of applicants' claimed compositions has not been shown to violate a scientific principle or law of nature. Applicants' specification provides clear and convincing evidence that the claimed antibodies provide protection from a lethal dose of bacteria in an *in vivo* mouse model. For example, Example 8 in the specification describes the injection of mice with H13C4 antibody (humanized anti Stx1B), mouse 13C4 antibody (anti Stx1B), or H11E10 (humanized anti-Stx2A). The mice were then challenged with crude Stx1 toxin protein and monitored. The antibodies to Stx1B protected the mice against at least 10 times the normal lethal toxin dose, while the negative control antibodies, directed to Stx2A protein did not provide such protection. These results plainly demonstrate the efficacy of the claimed antibodies in protecting the mouse from the lethal effects of Stx1.

Example 8 also describes the protection against oral infection with Stx2-producing enterohemorrhagic *Escherichia coli* (EHEC) bacterial strains. In this case, two different strains of mice were challenged with EHEC strains, each producing Stx2 protein. The mice were injected at day zero and again at day one with H11E10 antibody (humanized anti Stx2A), mouse 11E10 antibody (anti Stx2A), or mouse 13C4 (anti-Stx1B). Again, only the specific antibody, in this case the murine and humanized 11E10 antibodies, provided protection against the lethal dose of EHEC. These examples clearly

demonstrate that the antibodies of the invention are useful as a therapeutic for the treatment of diseases caused by Shiga toxin producing pathogens such as EHEC. Example 9 of the specification describes the use of the claimed antibodies for the treatment of diseases caused by bacteria producing Shiga toxin.

In short, applicants again note that no evidence is present in this case to doubt the objective truth of the statements found in applicants' specification. Moreover, applicants' specification does indeed demonstrate how the claimed pharmaceutical compositions are to be used, and presents compelling data demonstrating the in vivo efficacy of the claimed compositions. Accordingly, applicants request reconsideration and withdrawal of this basis for the enablement rejection.

Rejection under 35 U.S.C. § 112, second paragraph

Claim 20 was deemed vague and indefinite on the grounds that "the language used and the organization of the claim is unclear." This issue has been addressed by the present claim amendment.

Rejection under 35 U.S.C. § 103(a)

Claims 1, 2, 14, 17-20, 23, 29, and 32-43 were rejected under 35 U.S.C. § 103(a) as being unpatentable over Speirs et al. (*Canadian Journal of Microbiology*, 37:650-653, 1991; "Speirs") or O'Brien et al. (U.S. Patent No. 5,747,272;

"O'Brien") in view of Carter et al. (WO 94/04679; "Carter") and Shitara et al. (U.S. Patent No. 5,866,962; "Shitara"). Speirs and O'Brien are cited for disclosing the mouse 13C4 and 11E10 antibodies. Carter and Shitara are relied upon for disclosing methods of producing humanized antibodies. For the following reasons, this rejection should be withdrawn.

Applicants' application includes claims directed to various embodiments of a humanized monoclonal antibody that binds to Shiga toxin protein. Though the claims vary, independent claim 1 is perhaps most representative:

> 1. A humanized monoclonal antibody that binds to Shiga toxin protein, comprising a constant region and a variable region, wherein said constant region contains at least part of a human immunoglobulin constant region and said variable region contains at least part of an immunoglobulin variable region as shown in Figure 3 (SEQ ID NO: 21) or Figure 6 (SEQ ID NO: 42), wherein the antibody specifically reacts with Stxl or Stx2 antigen.

The Federal Circuit has stated:

> "[V]irtually all [inventions] are combinations of old elements." Therefore an examiner may often find every element of a claimed invention in the prior art. If identification of each claimed element in the prior art were sufficient to negate patentability, very few patents would ever issue. Furthermore, rejecting patents solely by finding prior art corollaries for the claimed elements would permit an examiner to use the claimed invention itself as a blueprint for piecing together elements in the prior art to defeat the patentability of the claimed invention. Such an approach would be "an illogical and inappropriate process by which to determine patentability." *In re Rouffet*, 149 F.3d 1350, 1357-58, 47 USPQ2d 1453, 1457 (Fed. Cir. 1998) (internal citations omitted).

Moreover, the court has explained that "[t]o prevent the use of hindsight based on the invention to defeat patentability of the invention, ... the examiner [is required] to

show a motivation to combine the references that create the case of obviousness." *In re Rouffet*, 149 F.3d 1350, 1357-58, 47 USPQ2d 1453, 1457 (Fed. Cir. 1998). Simply put, in order to establish a *prima facie* case of obviousness, "the examiner must show reasons that the skilled artisan, confronted with the same problems as the inventor and with no knowledge of the claimed invention, would select the elements from the cited prior art references for combination in the manner claimed." *In re Rouffet*, 149 F.3d 1350, 1357-58, 47 USPQ2d 1453, 1457 (Fed. Cir. 1998). As explained below, the examiner has failed to show a *prima facie* case of obviousness and the rejection should be withdrawn.

As motivation for combining the references of record, the examiner states that "it would have been ... obvious for one of skill in the art to employ the methodologies disclosed by Carter et al. to humanize the 13C4 and 11E10 antibodies in order to reduce the side effects associated with anti-mouse immunoglobulins since the process of humanizing a known antibody is well known in the art." There is, however, nothing in the references of record that provides any basis for selecting either the 13C4 or the 11E10 as a candidate antibody for humanization.

Why select the Speirs and O'Brien antibodies for humanizing along the lines described by Carter or Shitara? Speirs and O'Brien describe using the mouse 13C4 and 11E10 antibodies for detecting cytotoxins. The examiner assumes that the ability of the mouse 13C4 or 11E10 antibodies to detect cytotoxins may be equated with treating a patient. There is nothing in Speirs or O'Brien that teaches, suggests, or motivates the

skilled worker to use their antibodies to treat a shiga toxin induced disease, much less a teaching to administer these antibodies to a patient. Accordingly, there is no motivation "to employ the methodologies disclosed by Carter et al. to humanize the 13C4 and 11E10 antibodies in order to reduce the side effects associated with anti-mouse immunoglobulins." Carter and Shitara simply describes methods for humanizing an antibody, and each fails to describe or even mention either the 13C4 or 11E10 antibody. Furthermore, the examiner fails to explain, when analyzing the references, "what specific understanding or technical principle .... would have suggested the combination." *See Rouffet*, 149 F.3d at 1357, 47 USPQ2d at 1459. Accordingly, to the extent that the examiner relies upon Speirs and O'Brien to establish that it would have been obvious to use the 13C4 or 11E10 antibodies as a therapeutic composition to treat a disease, merely because it would be obvious to try such an experiment, the examiner is in error. *See Hybritech Inc. v. Monoclonal Antibodies, Inc.* 802 F.2d 1367, 1380, 231 U.S.P.Q. 81, 91 (Fed. Cir. 1986) *cert. denied*, 480 U.S. 947 (1987). ("Obvious to try" is improper consideration in adjudicating obviousness issue.)

A reference-by-reference, limitation-by-limitation analysis, as presented in the Office Action, fails to demonstrate how the Speirs, O'Brien, and Carter references teach or suggest their combination with the murine 13C4 or 11E10 antibodies, used to detect a cytotoxin, to yield the claimed humanized antibody compositions. The obviousness analysis in the Office Action is limited to a discussion of how the references can be

pieced together, in hindsight, to yield the claimed invention. It is an error to reconstruct the patentee's claimed invention from the prior art by using the patentee's claim as a "blueprint." As the Federal Circuit stated in *Interconnect Planning Corp. v. Feil*, 774 F.2d 1132, 1143, 227 U.S.P.Q. 543, 551 (Fed. Cir. 1985):

> When prior art references require selective combination to render obvious a subsequent invention, there must be some reason for the combination other than the hindsight gleaned from the invention itself. There must be "something in the prior art as a whole to suggest the desirability, and thus the obviousness, of making the combination. [citations omitted.]

To believe that one skilled in the art would be motivated to make applicants' claimed humanized antibodies, when Speirs, O'Brien, and Carter, either alone or in combination, never even discuss, suggest, or mention modifying the mouse 13C4 or 11E10 antibodies used for detecting cytotoxins in a way that would lead one to applicants' claimed humanized antibody compositions is to assume a level of inspiration constituting inventive activity. The case law makes clear that to avoid a hindsight-based obviousness analysis that the Patent Office bears the burden of elucidating factual teachings, suggestions, or incentives from the prior art that show the suitability of the combination of references. *See Graham v. John Deere Co.*, 383 U.S. 1, 18, 148 U.S.P.Q. 459, 467 (1966) ("strict observance" of factual predicates to obviousness conclusion required).

Absent a motivation to combine references, the examiner has not shown a proper *prima facie* case of obviousness, and the rejection of the claims under § 103 for obviousness over Speirs or O'Brien in view of Carter or Shitara should therefore be

withdrawn.

CONCLUSION

Applicants submit that the pending claims are in condition for allowance and such action is respectfully requested.

Enclosed is a Petition to extend the period for filing an Appeal Brief for five months, to and including October 22, 2004. Applicants further enclose a check for $108.00 in payment of new claims 44-55.

If there are any additional charges or any credits, please apply them to Deposit Account No. 03-2095.

Respectfully submitted,

Date: 22 October 2004

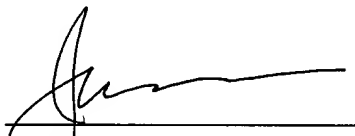

James D. DeCamp, Ph.D.
Reg. No. 43,580

Clark & Elbing LLP
101 Federal Street
Boston, MA 02110
Telephone: 617-428-0200
Facsimile: 617-428-7045

Molecular Immunology, Vol. 30, No. 4, pp. 369–377, 1993
Printed in Great Britain.

0161-5890/93 $6.00 + 0.00

CHARACTERIZATION OF AN ANTI-DIGOXIN ANTIBODY BINDING SITE BY SITE-DIRECTED *IN VITRO* MUTAGENESIS*

RICHARD I. NEAR,†‡ MEREDITH MUDGETT-HUNTER,† JIRI NOVOTNY,§‖ ROBERT BRUCCOLERI§‖ and SHI CHUNG NG§‖

†Cellular and Molecular Research Laboratory, Massachusetts General Hospital and Department of Medicine, Harvard Medical School, Boston, MA 02114, U.S.A.; and §Bristol-Myers Squibb Pharmaceutical Research Institute, Princeton, NJ 08543, U.S.A.

(*Received* 24 *April* 1992; *accepted* 9 *August* 1992)

Abstract—*In vitro* mutagenesis and immunoglobulin gene transfection were used to investigate the binding site of a monoclonal antibody, 2610, that binds to digoxin, a cardiac glycoside. A computer model was generated in order to select sites in the complementarity determining regions (CDR) that would participate in binding. Residues in the CDR segments were chosen that possess high solvent exposure and were located in a putative cleft. The cloned heavy and light chain variable regions were subjected to *in vitro* mutagenesis at these sites. The mutated variable regions in M13 were then subcloned into expression vectors and transfected. The affinities and specificity binding properties of the resultant expressed antibodies were measured. Many of the mutants of the putative contact residues showed significant but not major alterations of binding properties. Since most of the residues in the binding site are non-polar and aromatic and since many of the mutations resulted in only modest binding changes, we theorize that much of the high affinity binding ($>10^9$/M) is the cumulation of many weak interactions, arising from dispersion forces and hydrophobic effects in the pocket. Preliminary mutagenesis of two L chain positions proposed to bind to the lactone end of digoxin have larger binding effects. Specificity studies show that the mutants more frequently possess altered binding to the lactone ring of digoxin that altered binding to other digoxin moieties. The data are most suggestive of a model in which lactone is at the bottom of a binding pocket, followed by the steroid nucleus and then by the sugar moiety extruding out of the pocket. The binding information may be useful in understanding the immune response to large, hydrophobic haptens.

INTRODUCTION

Digoxin is a cardiac glycoside which is uncharged and contains a steroid nucleus, a lactone ring and three sugar residues. Antibodies to digoxin provide a useful and relatively unique model for antibody–hapten interaction since: (1) digoxin is unusually large for a hapten and occupies most of the antibody combining site (Brunger, 1991; Kabat, 1966); (2) X-ray crystallographic structures of digoxin and several analogs are known and show that the cardiac glycoside steroid ring is conformationally rigid, regardless of functional group substitutions (Go *et al.*, 1980); (3) there is ample availability of many digoxin analogs for the investigation of fine specificity of antigen (Ag) binding (Fieser and Fieser, 1959); and (4) several monoclonal anti-digoxin antibodies generated from immunized A/J strain mice are available and have unusually high affinities (greater than 10^9/M) and different fine specificity patterns (Mudgett-Hunter *et al.*, 1982, 1985). The combination of these high affinities and varying specificity patterns suggests that multiple antibody–antigen contacts exist within the antibody combining sites and that these antibodies recognize digoxin in a different fashion with different binding sites (Mudgett-Hunter *et al.*, 1985). The immunology of a hapten this large that induces antibodies with such high affinity has only been minimally studied (Mudgett-Hunter *et al.*, 1982, 1985; Bates *et al.*, 1985). Such an immune response might represent a different antibody response than that to most small haptens and may occur through unknown affinity maturation steps. To understand such a response it is essential to initially understand the antigen–antibody interactions involved.

Previously we have described sets of monoclonal anti-digoxin antibodies that share homologous H and L chains (Mudgett-Hunter *et al.*, 1985; Near *et al.*, 1991;

*This work was supported by National Institutes of Health Grant HL19259.

‡Author to whom correspondence should be addressed at: Cellular and Molecular Research Laboratory, Massachusetts General Hospital, Boston, MA 02114, U.S.A.

‖Current address: Bristol-Myers Squibb Pharmaceutical Research Institute, P.O. Box 4000, Princeton, NJ 08543, U.S.A.

Abbreviations: VH, heavy chain immunoglobulin variable region; VL, light chain variable region; Vκ, kappa light chain variable region; H, heavy chain; L, light chain; kb, kilobase; CDR, complementarity determining region; CPM, counts per minute; PBSA, PBS containing 0.10% sodium azide; PCR, polymerase chain reaction. Mutations are abbreviated as indicated by first noting L or H chain, the position in consecutive numbering, and the single letter amino acid mutation from the first amino acid to the second amino acid (i.e. H104W:F).

Near and Haber, 1989; Panka and Margolies, 1987). These sets are useful in structure–function studies because the small mutational sequence differences are responsible for binding alterations. This allows the assignment of particular protein residues to certain contributions of Ag binding. We cloned and expressed the genes from one of these sets (the 35-20 set that does not contain a major idiotype). By expressing various combinations of H and L chain in transfectomas, we were able to show that VH mutations control the fine specificity properties that distinguish different members of this set. Specifically, two CDR2 residues control the characteristic binding properties that distinguished the antibodies in the set. By *in vitro* mutagenesis we were able to alter Ag specificity without affecting affinity (Near *et al.*, 1991). A computer model was generated which was consistent with the data.

However, some anti-digoxin antibodies with interesting binding properties are relatively unique in V region sequences. One such antibody, 26-10, has a unique H chain, yet contains a L chain that is homologous with those of four other antibodies (Mudgett-Hunter *et al.*, 1985; Near *et al.*, 1990). Antibody 26-10 is insensitive to removal of the sugar moieties, removal of the 12-hydroxy group but very sensitive to substitution of the lactone of digoxin. These binding properties distinguish 26-10 from the other anti-digoxin antibodies (Mudgett-Hunter *et al.*, 1985; Schildbach *et al.*, 1991). Aside from its binding properties, 26-10 is of interest because an X-ray structure will soon be available (Brunger, 1991; Jeffrey and Sheriff, personal communication). Since the 26-10 H chain is unique among the anti-digoxin antibodies available, the various binding properties of this antibody could not be readily assigned to certain residues by comparing the 26-10 protein sequence to those of homologous antibodies. Therefore, we generated a computer model in order to estimate positions that would be informative in mutagenesis experiments. Here we describe the mutagenesis of 26-10 H and L chain variable region protein residues in order to characterize the digoxin binding site of 26-10 and the type of antibody–antigen interactions involved.

MATERIALS AND METHODS

Cell lines

The anti-digoxin hybridoma 26-10 (γ2a, κ) has been previously described (Mudgett-Hunter *et al.*, 1982, 1985). The cell line 26-10 κ is a H chain-loss variant of 26-10 which was selected by simply subcloning 26-10 and assaying subclones for loss of γ2a by an ELISA assay and was found not to produce 26-10 H chain mRNA or any measurable digoxin-binding protein (Near, unpublished experiments). The cell line 26-10 Hwt was produced by transfecting J558L (λ) (kindly donated by S. Morrison, U.C.L.A., Los Angeles, CA 90607) with the unmutated 26-10 H chain expression vector. This cell line produces a 26-10 H chain and J558 lambda chain (confirmed by ELISA for γ2b) which does *not* bind digoxin (Near, unpublished experiments). The cell line 26-10 wt was produced by transfecting both the unmutated 26-10 H and L chain expression vectors into J558L. This line binds digoxin with the same binding properties as 26-10 itself (see Results). All cells were maintained in Dulbecco's modified Eagle's medium supplemented with 15% fetal calf serum (GIBCO, Grand Island, NY), 50 μg/ml gentamicin sulfate (GIBCO), and 0.6 mg/ml L-glutamine.

Expression constructs

The expression vector, pX_{VH}, for the expression of VH has been previously described (Near *et al.*, 1991). This vector was usually transfected into the cell line 26-10 κ. Briefly, pSV2gpt vector (Mulligan and Berg, 1980) was modified to contain a polylinker and a murine γ2b genomic fragment. For expression, the mutated VH26-10 XbaI 1.7 kb genomic fragment (Near *et al.*, 1990) was subcloned from M13 to the expression vector in the correct orientation. The 26-10 Vκ expression vector, pX_κ, has also been previously described (Near, 1992) and was usually transfected into the cell line 26-10 Hwt. Briefly, the 27 kb HindIII–XbaI genomic Vκ fragment (Near *et al.*, 1990) was altered such that the HindIII site was changed to an EcoRI site by an adaptor and then subcloned into M13mp18 for mutagenesis. For expression, the 26-10 Vκ mutated EcoRI–XbaI 2.7 kb piece was then subcloned into pSV2neo (Southern, 1982) into which the 5.6 kb EcoRI–BamHI genomic 40-140 Vκ Cκ piece (Near *et al.*, 1991) had been cloned and the EcoRI–XbaI 40-140 Vκ has been removed.

DNA transfection

The construct for antibody expression was transfected into cells with a Gene-Pulsar electroporation apparatus (Bio-Rad Laboratories, Richmond, CA) as previously described (Near *et al.*, 1991). After 48 hr in normal media, cells were placed in selection media. For VH with gpt gene selection, cells were plated into 96-well plates in 0.4 μg/ml mycophenolic acid, 250 μg/ml xanthine, and 15 μg/ml hypoxanthine in normal medium. For Vκ selection with the neo-gene, the selection media contained 1.5 mg/ml G418 (GIBCO BRL, Gaithersburg, MD).

In vitro *mutagenesis*

Mutagenesis was done as described by Kunkel (1985) with a Muta-Gene *in vitro* mutagenesis kit (Bio-Rad Laboratories, Richmond, CA). The 1.7 kb XbaI VH fragment or the 2.7 kb EcoRI–XbaI Vκ fragments were cloned into M13 and phage grown in CJ236 to obtain uridinylated template. Oligonucleotides were annealed to the template, second strand synthesized and the products transfected into MV1190 according to the manufacturer. All mutated V regions were sequenced to confirm correct mutagenesis. The sequences of oligonucleotides used for mutagenesis will be supplied upon request.

DNA sequence determination

The V regions were sequenced by the dideoxy chain-termination method (Sanger *et al.*, 1977) using Seque-

nase (United States Biochemicals, Cleveland, OH) and adenosine 5′-[γ-^{35}(S)thio] triphosphate (Amersham, Arlington Heights, IL) with M13 phage DNA. The sequences of the oligonucleotide primers will be supplied on request.

Antibody affinity determination

The affinity constant was determined by a double precipitation assay as described (Mudgett-Hunter *et al.*, 1985). Briefly, supernatant from each transfectoma was diluted in 1% horse serum in PBSA to a concn estimated to be at the level of the kD or lower. This diluted supernatant was incubated with different concns of [^{3}H]digoxin (25 μCi/mmol, New England Nuclear, Boston, MA) overnight at 4°C. The Ag–Ab complex was precipitated with rabbit anti-mouse IgG (ICN Immunobiologicals Inc., Lisle, IL) overnight followed by goat anti-rabbit IgG (kindly donated by Dr Charles Homey, Massachusetts General Hospital, Boston, MA) for 4 hr at 4°C. The precipitate was collected onto glass fiber filters (24 mm, Schlechter and Schuell, Keene, NH); the filters were placed into 5 ml of scintillation fluid (Ultima Gold, Packard Instrument Co., Sterling, VA) and counted in a Packard 1500 Tri-Carb Liquid Scintillation Analyzer (Packard Instrument Co., Sterling, VA). The data were analyzed with the program LIGAND (Munson and Robard, 1980) which calculates K_a and the antibody concn.

Binding specificity determination

The fine specificities of the anti-digoxin antibodies from cell supernatants were determined by measuring the competition between digoxin and its analogs in an RIA as previously described (Mudgett-Hunter *et al.*, 1985; Near *et al.*, 1990, 1991). Briefly, 96-well plates previously coated with affinity-purified goat anti-mouse F(ab′)2 (ICN Immunobiologicals Inc., Lisle, IL) were incubated with transfectoma cell supernatants at 4°C overnight. The plates were washed and then dilutions of non-radioactive cardiac glycoside competitors (10^{-10}–10^{-4} M) in PBSA containing 1% horse serum and 5% ethanol were added to the wells followed immediately by 50,000 cpm of [^{125}I]-digoxin (Cambridge Medical Diagnostics, Burlington, MA) added to the same wells. The competition mix was allowed to incubate at 4°C overnight. Plates were then extensively rinsed and wells were counted (Micromedic Systems Automatic Gamma Counter, Model 4/6000, INC Biomedicals Inc., Costa Mesa, CA). For each antibody, ability of an analog to compete was determined by comparing the amount of unlabeled analog required to achieve 50% inhibition relative to the amount of unlabeled digoxin needed for 50% inhibition of [^{125}I]-digoxin binding. Antibody isotypes were determined to confirm appropriate transfection and expression with the Mouse Ig Subtype Identification Kit (Boehringer Biochemicals, Indianapolis, IN).

Computer-generated model

Prior to commencing mutagenesis experiments, we constructed a model of the Fv of 26-10. Briefly, the protocol developed for the reconstruction of McPC603 and HyHEL5 (Bruccoleri *et al.*, 1988) was used to construct the model of the 26-10 binding site. In this construction, we began with the X-ray crystal structure of McPC603 (Satow *et al.*, 1986). The V region sequences of 26-10 was aligned with those of McPC603, and conformational searches using CONGEN (Bruccoleri and Karplus, 1987) were performed on the sidechains in the framework with different sequence. Then the loops of the antibody were constructed in sequence starting with loops closest to the framework and ending at the tip of the combining site residue, except that the H1 backbone was taken directly from McPC603 because of the high sequence similarity. The specific order and amino acid residues constructed by conformational searches were L2 (55–60), L3 (94–101), H2 (49–57), H3 (98–106), and L1 (31–38).

The computer model showed a cleft of the proper dimensions to bind digoxin. Residues for mutagenesis were selected based upon their position with respect to the cleft and their surface accessibility (Table 1). No attempts were made to use the 26-10 computer model for detailed atomic interpretation of digoxin binding. Our previous work has shown (Bruccoleri *et al.*, 1988) that computer modeling, although often capable of reproducing overall shapes of binding sites, is not accurate enough for such detailed studies. Therefore, the computer model was used solely to choose sites for mutagenesis. Further refinements of this model are underway and will be published in comparison with the X-ray structure in a later paper (Bruccoleri and Novotny, unpublished experiments); however, further details of the computer model used in this work will be supplied upon request. Since the X-ray structure has been recently solved and will be published shortly (Sheriff and Jeffrey, personal communication), we discuss many of the results in terms of structural correlates with the crystallographic structure (see Discussion).

RESULTS

Sites selected for mutagenesis

A computer model was used to estimate which sites to subject to *in vitro* mutagenesis. The criteria used for the choice of mutated positions were location in the CDR regions, high surface accessibility and participation in a putative antigen-binding cleft. Figure 1 shows the heavy and light-chain 26-10 sequences and the residues chosen for mutagenesis. Table 1 shows the surface accessibility of the residues in the CDR areas as calculated from the computer model. The computer model (Materials and Methods) predicted a cleft into which the digoxin might closely fit. Although recent crystallographic data differ from the computer model in many respects (see Discussion), the model was still practicable since many of the mutated sites contribute to antigen binding as shown in the crystal structure (Sheriff and Jeffrey, personal communication). Mutations were chosen on the basis of all three criteria with priority given to participation in the putative antigen-binding cleft. The model predicted that,

Table 1. Surface accessibility of CDR residues [Å²][a]

Heavy chain CDRs									
CDR1									
ASP31	PHE32	TYR33	MET34	ASN35					
49.0	44.5	81.2	0.4	5.0					
CDR2									
TYR50	ILE51	SER52	PRO53	TYR54	SER55	GLY56	VAL57	THR58	GLY59
32.2	3.1	6.1	21.5	127.5	70.8	87.5	70.5	59.0	13.5
TYR60	ASN61	GLU62	LYS63	PHE64	LYS65	GLY66			
41.7	21.4	103.7	84.6	0.6	123.5	76.5			
CDR3									
SER99	SER100	GLY101	ASN102	LYS103	TRP104	ALA105	MET106	ASP107	TYR108
0.0	22.9	74.1	28.2	36.1	57.3	7.3	6.5	10.6	83.7
Light chain CDRs									
CDR1									
ARG24	SER25	SER26	GLN27	SER28	LEU29	VAL30	HIS31	SER32	
87.5	1.4	69.6	106.9	66.2	0.1	64.9	51.4	133.6	
ASN33	GLY34	ASN35	THR36	TYR37	LEU38	ASN39			
145.3	43.9	50.0	11.1	53.9	1.8	3.1			
CDR2									
LYS55	VAL56	SER57	ASN58	ARG59	PHE60	SER61			
51.5	102.0	61.0	113.0	74.4	50.3	93.3			
CDR3									
SER94	GLN95	THR96	THR97	HIS98	VAL99	PRO100	PRO101	THR102	
0.01	0.04	7.3	27.8	49.8	65.4	33.3	6.9	28.2	

[a]Surface accessibility calculated in the computer program CONGEN (Bruccoleri and Karplus, 1987).

for L chain, L2 would not be involved, L1 would be minimally involved and L3 would form significant contacts with the hapten. For H chain, all three CDR areas would be involved with H2 and H3 being the primary contributors and H1 a minimal contributor. Since priority was given to residues that would be present in the putative cleft, some residues with high surface accessibility were not mutated. Position L101P was mutated since we had data indicating that this was one of the positions differing between antibody 26-10 and 40-100 responsible for much of their binding differences (Near, unpublished experiments). These constraints limited the number of sites for mutagenesis to those shown in Fig. 1. Most mutations were of semi-conservative nature in order to produce a significant effect without producing global structural alterations.

Genetic constructs express a 26-10 binding site

The genetic constructs that express 26-10 H and L chains are similar, though not identical, to those previously described (Near *et al.*, 1990). When the previous H and L chain constructs were both transfected into the cell line J558L (producing only λ chain), they expressed an antibody with binding properties indistinguishable from that of the 26-10 antibody (produced by the original hybridoma). This experiment was repeated here with the present 26-10 H and L constructs (Materials and Methods). Tables 2 and 3 show that the affinity and

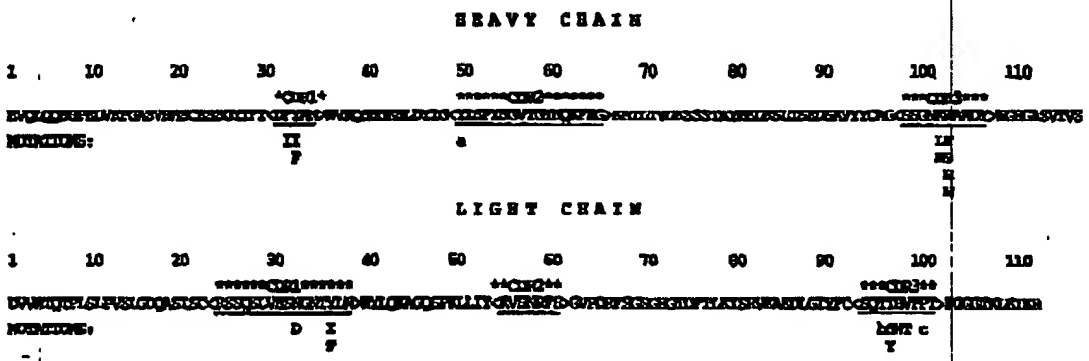

Fig. 1. Protein sequences and sites of mutagenesis for 26-10 H and L chain V regions. The numbering is sequential from the start of the mature protein. The sequences have been previously described (Near *et al.*, 1990). The CDR segments are shown and the sites of mutagenesis are noted below the sequence. (a) Position H 50 mutation Y to H has been previously described (Schildbach *et al.*, 1991). (b) and (c) Positions L96 T:G and L101 P:L mutations will be detailed in another paper (Near, unpublished experiments).

Table 2. Fine specificities of 26-10 mutants relative to 26-10[a]

Antibody	Digoxigenin	Digitoxin	Digitoxingenin	Gitoxin	Acetylsrophanthidin	Ouabain	Dihydrodigoxygenin
26-10	1.1	1.2	1.5	11	3.0	47	523
26-10 wt[b]	1.2	2.1	2.7	6.4	2.2	28	653
Heavy chain mutants							
H32 F:I	0.8	1.6	1.5	8.6	3.0	58	490
H33 Y:I	0.6	1.6	2.3	4.8	2.1	8.3[c]	23
H33 Y:F	1.0	1.6	2.1	5.0	1.8	48	230
H50 Y:H[d]			Significantly different fine specificity (see text)				
H103 K:L	1.2	1.6	2.4	4.6	1.1	18	304
H103 K:M	0.5	2.7	1.6	5.2	2.3	18	102
H104 W:F	1.0	1.5	1.6	8.0	4.1	57	165
H104 W:S	1.2	1.0	1.0	9.8	1.7	27	380
H104 W:H	1.2	2.1	2.4	34	8.5	56	255
H104 W:N	0.8	1.7	1.2	15	2.9	33	584
Light chain mutants							
L33 N:D	0.8	1.4	1.3	3.7	1.6	9.2	80
L37 Y:I	1.7	0.8	1.0	4.3	1.5	14	61
L37 Y:F	0.8	1.5	1.7	2.8	1.9	24	525
L97 T:S	1.0	1.5	1.2	4.3	2.1	14	213
L97 T:Y	1.8	1.2	1.3	2.4	0.9	37	140
L98 H:W	0.7	1.3	0.8	19.2	1.5	25	72
L99 V:T	1.2	1.4	1.2	21.5	2.7	25	78
L96 T:G[e]			Large differences in specificity and large affinity loss (see text)				
L101 P:L[e]			Large differences in specificity and large affinity loss (see text)				

[a]Concentration of inhibitor relative to digoxin yielding 50% inhibition of [^{125}I]-digoxin binding. The concn of cold digoxin that inhibits at 50% was set at 1.0.
[b]26-10 wt is the transfectoma expressing both H and L 26-10 constructs (see text).
[c]Underscored numbers are specificities greater than two-fold different than unmutated 26-10.
[d]Mutation H50Y:H was previously published (Schildbach *et al.*, 1991).
[e]Mutations at L96 and L101 will be published later in relation to the differences between antibody light chains of 26-10 and 40-100 (see text; Near, unpublished experiments).

fine specificities of the new recombinant transfected antibody, 26-10 wt, again are experimentally indistinguishable from the original 26-10 antibody. (The antibody from cell line 26-10 Hwt, containing the 26-10 H construct transfected into J558L, does not bind digoxin.)

Affect of mutagenesis on antigen specficity

Table 2 shows the fine specificity profiles measured by the ability of digoxin analogs to compete with digoxin in a competitive RIA. Unmutated 26-10 binds dihydrodigoxigenin, containing an altered lactone ring, with

Table 3. Affinities of 26-10 mutants

Heavy chain mutants		Light chain mutants	
Antibody	Affinity[a]	Antibody	Affinity
H32 F:I	$4.8 (\pm 1.5) \times 10^9$	L33 N:D	$2.8 (\pm 0.4) \times 10^9$
H33 Y:I	$2.2 (\pm 0.1) \times 10^8$	L37 Y:I	$2.0 (\pm 0.2) \times 10^8$
H33 Y:F	$1.6 (\pm 1.0) \times 10^9$	L37 Y:F	$2.9 (\pm 0.8) \times 10^9$
H50 Y:H[b]	$6.4 (\pm 0.9) \times 10^8$	L97 T:S	$6.0 (\pm 1.0) \times 10^9$
H103 K:L	$3.7 (\pm 0.8) \times 10^9$	L97 T:Y	$1.3 (\pm 0.2) \times 10^9$
H103 K:M	$3.5 (\pm 0.4) \times 10^8$	L98 H:W	$2.3 (\pm 0.6) \times 10^9$
H104 W:F	$4.2 (\pm 0.5) \times 10^8$	L99 V:T	$4.5 (\pm 0.8) \times 10^9$
H104 W:S	$2.9 (\pm 0.3) \times 10^8$	L96 T:G[c]	Large affinity loss
H104 W:H	$8.6 (\pm 0.6) \times 10^9$	L101 P:L[c]	Large affinity loss
H104 W:N	$8.2 (\pm 0.4) \times 10^8$		
Hybridoma	26–10	$4.2 (\pm 0.4) \times 10^9$	
Trahsfectoma	26–10 wt	$4.4 (\pm 0.4) \times 10^9$	

[a]The average intrinsic affinity constant (K_o, M^{-1}) and error were calculated according to the algorithm LIGAND (Materials and Methods).
[b]H50 Y:H previously published (Schildbach *et al.*, 1991).
[c]Near, unpublished experiments.

at least 20-fold lower affinity *relative* to the other analogs tested on the same antibody, although there is some loss of binding to ouabain and acetylstrophanthidin which have substitutions on the β surface of steroid rings A and B. Many of the 26-10 mutations resulted in little effect on specificity as compared with unmutated 26-10 antibody. In the cases where a mutation affects specificity, there is often, but not always, a concomitant change in affinity. The mutations affecting specificity result in changes of binding to dihydrodigoxigenin more often than to the other analogs. Mutations at 10 of the 12 positions selected in Fig. 1 result in antibodies that have altered lactone binding (Table 2). This effect is especially prevalent in L chain since all seven of the L chain positions mutated result in changes in lactone binding. The observation that binding to dihydrodigoxigenin is affected by mutagenesis more often than is binding to the other analogs that contain a normal lactone ring suggests that lactone participates in multiple or strong interactions with the 26-10 binding site. The other areas of the digoxin molecule may have fewer or weaker interactions, consistent with the result that fewer mutations were able to alter binding to digoxin moieties other than lactone.

Unmutated 26-10 does not distinguish between congeners with and without (the "genins") the digitoxose groups (Table 2) (Mudgett-Hunter *et al.*, 1985), suggesting that this end of the molecule participates minimally in binding. The mutant antibodies also show no sensitivity to the presence of the digitoxose sugars. Mutation H50Y:H shows some sensitivity to lactone ring substitutions, but more sensitivity to substitutions at the 12 and 16 positions (rings C and D) (Schildbach *et al.*, 1991). Mutation at positions L96T:G and L101P:L (which will be reported elsewhere in detail) show marked changes: The L101P:L mutation lowers digoxin affinity about 200-fold and the L96T:G mutation lowers binding by about 100-fold (Near, unpublished). Both of these L chain mutations show more than two orders-of-magnitude loss of sensitivity to the lactone substitution in dihydrodigoxigenin and much smaller changes in recognition of substitution at the 12 position. They show essentially no change of specificity for ouabain or acetylstrophanthidin, which contain substitutions on the β surface of steroid rings A and B, and no sensitivity to lack of sugar moieties. In summary, the results would be consistent with a binding pocket which binds lactone most strongly (possibly at the bottom of a pocket), binds the steroid nucleus with intermediate strength and does not bind sugar at all (possibly extending out of a pocket).

Affect of mutagenesis on antigen affinity

Table 3 shows the affinity constants for the recombinant antibodies containing the mutations. Again, we find that most mutations have relatively little effect on affinity. However, mutations at six positions are noteworthy since they produce significant loss of affinity (Table 3); H33Y:I, H50Y:H [a mutation previously described (Schildbach *et al.*, 1991)], H104W (four mutations), L37Y:I, L96T:G and L101P:L. The two mutations in L chain, L96T:G and L101P:L (Near, unpublished experiments), actually decrease affinity by about 100- and 200-fold, respectively, although some of this large magnitude of affinity loss could be due to the non-conservative nature of these mutations. In all cases in which affinity is lowered by mutagenesis there is also altered binding to dihydrodigoxygenin; however, there are several cases where altered binding to dihydrodigoxygenin does not mean lower affinity. Since the loss of digoxin affinity in the mutated antibodies seems most often to be correlated with diminished ability to distinguish digoxin from the lactone congener dihydrodigoxigenin, the antibody may snugly fit around the lactone ring and/or have multiple or strong interactions with the lactone ring. These interactions may be relatively more important in determining affinity. We did not find any change in aglycone binding associated with change in affinity, suggesting that the sugar groups are not highly participating in the binding.

Model for the binding site

We regarded the computer-built model of the binding site as approximate, and we limited its use to identification, as confirmed by mutagenesis, of the most prominent surface-exposed side chains in the CDR regions. Since digoxin contains a rigid steroid backbone composed of four fused, aliphatic cyclohexane rings in chair conformations and a planar lactone ring and since the binding constant is high [-11.5 kcal, calculated by $\Delta G = RT \ln K$ (Novotny *et al.*, 1989)], we expected extensive surface binding contacts with most of the binding energy derived from hydrophobic effects and dispersion forces. The impact of replacing a hapten-contacting amino acid by mutagenesis was expected to be proportional to the difference in surface areas of the two side chains, provided that no serious steric clash had been introduced into the mutant. Also, since each single side chain contributes but a fraction of the total hapten-contacting surface (Table 1), most single-residue mutations should have modest effects on the equilibrium binding constant. The binding data have mostly born out the above assumption. The exceptions are the L96T:G and L101P:L mutants which may be binding to the lactone via interactions other than hydrophobic bonds or may be changing the overall conformation of the binding site since these are non-conservative mutations (Near, unpublished experiments). For example, H104W has, in the crystal structure (Sheriff and Jeffrey, personal communication), some 78 Å^2 of solvent-exposed surface (the computer model estimates 57 Å^2) and, if all of this surface would be available to be in contact with the hapten, the side chain would contribute some -2 kcal of binding energy, i.e. $\approx$17% total (Chothia, 1974; Novotny *et al.*, 1989). Indeed, when H104W is replaced by a smaller side chain such as Ser, Asn, or His, the resulting binding energy differences ($\Delta\Delta G$) were in the range of 1–2 kcal (specifically 1, 1.8 and 1.4 kcal, respectively). The mutagenesis results were also useful in suggesting the orientation of the hapten in

the binding site. Since, in the mutated antibodies, the binding to the lactone ring is highly altered, binding to the steroid nucleus moderately affected, and binding to the sugar moieties is not affected (Table 2), a longitudinal cleft model does not readily concur with the data. Rather, a binding pocket with lactone at the bottom, the steroid nucleus in the center and the sugar group extruded out from the pocket would be favored, as seen in the crystallographic structure.

DISCUSSION

Digoxin, a cardiac glycoside, possesses some relatively unique properties as a hapten since it is capable of occupying the entire antigen binding site (see Introduction). This may be reflected in the unusually high affinities of many monoclonal anti-digoxin antibodies (greater than 10^9/M for 26-10). One other hapten, fluorescein, is of similar large size but is also highly aromatic. The crystallographic structure of antibody 4-4-20 that binds fluorescein with high affinity is known (Herron *et al.*, 1989). In this structure there are 68 pairwise atomic interactions of which 42 are associated with the xanthonyl group and 26 with the benzoyl group. This differs from the smaller haptens such as phosphoryl choline or arsonate that overall participate in less contact with the surface of the binding site (Satow *et al.*, 1986; Rose *et al.*, 1990; Strong *et al.*, 1991). The authors have noted that the xanthonyl group is the immunodominant portion of this hapten. The xanthonyl ring is located deeper in the slot than the benzoyl group and has more interactions with the antibody. Further, it is noted that the fluorescein lies in a slot lined by residues of both the heavy and light chains. However, since fluorescein, unlike digoxin, is charged, the antibody residues are interacting in part with this charge as well as with aromatic interactions. Interestingly, the light chain of 4-4-20 is highly homologous with the light chain (but not the H chain) of another anti-fluorescein antibody, 04-01, which binds fluorescein in a probable different binding site and with different specificity properties (Bedzyk *et al.*, 1989). Also, interestingly, the L chain of 26-10 is very homologous (94%) with the L chain of 4-4-20. This light chain is also homologous with that of four other anti-digoxin antibodies which also share homologous H chains, 40-20, 40-60, 40-90 and 40-100 (Hudson *et al.*, 1990). It is unknown whether this common light chain may have some selective advantage in binding to large, aromatic or hydrophobic haptens.

The computer model of 26-10 suggested a cleft into which digoxin would fit, potentially interacting with the prominent exposed surface of residue H104W and the other residues indicated in Fig. 1. Many of the sites selected for mutagenesis (including the H104W mutants) resulted in significant binding changes, although of lower magnitude than we had predicted. Since most of the binding changes are not of large magnitude, much of the overall high affinity of 26-10 may be from the accumulation of many "weak" interactions. Recently crystallographic data has become available depicting the structure of 26-10 (Sheriff and Jeffrey, personal communication). The crystallographic data show that digoxin does not lie in a groove, but rather fits, lactone-end first, into a pocket with the sugar moiety exposed to the solvent and not participating in the binding. In general the mutagenesis results are consistent with the crystallographic data. Most of the residues predicted by the computer model do participate in binding, although the topology of the binding cleft in our model was different from that shown in the crystal structure. The crystal structure shows that position H104W interacts with rings B and C and the lactone ring, although the interaction with lactone is minimal. The loss of affinity upon mutation at this site may reflect change of the "snugness" of fit in the binding pocket (steric effects) as well as loss of interactions (mostly hydrophobic interactions). Since the binding is not at the bottom of the pocket and the type of interactions are not strong, this would be consistent with the data which shows that only about 10-fold affinity is lost and that the changes in specificity are not great (although there is some change in dihydrodigoxygenin binding). The binding of H104W:H shows significant loss of binding to gitoxin, an analog which has lost 12 hydroxy (ring C) and has gained 16 hydroxy (ring D). The mechanism for this altered specificity is not known, but consistent with H104 binding to the steroid nucleus. Position L37Y which affects specificity and affinity to about the same degree as H104, does not contact digoxin at all, but stacks directly in back of H104W (Sheriff and Jeffrey, personal communication). Therefore, position L37Y supports the position of H104W itself; mutation here produces an affinity change as if position H104 was mutated. The crystal structure shows that positions L96T and L101: both bind directly to the lactone ring at the bottom of the pocket and mutations here result in large changes in affinity and specificity (Near, unpublished experiments). Position H50Y binds to rings A, C and D, but not to lactone. Mutations at H50 show some alterations of specificity to the lactone ring, but much more sensitivity to substitutions at the 12 and 16 positions (rings C and D) and about 37-fold loss of affinity compared with unmutated 26-10 (when affinity of 26-10 and H50Y:H is measured by Schildbach in a different affinity assay) (Table 2) (Schildbach *et al.*, 1991).

Other mutations show significant alterations of lactone binding. Position H33Y interacts with rings A, B and D (and not directly with lactone), but mutation H33Y:I shows about a 20-fold loss of ability to distinguish dihydrodigoxigenen from digoxin. Mutations L33N:D (which shows no loss of affinity), L37Y:I, L97T:Y, L98H:W, L99V:T, L96T:G and L101P:L all significantly lessen the ability of 26-10 to distinguish dihydrodigoxigenin from digoxin. The contribution of L chain, especially LCDR3, to lactone binding is quite prominent. In addition to van der Waal interactions, hydrogen bonding and electrostatic interactions may be involved with lactone ring binding.

There are mutations that result in no loss of affinity. The sites of these mutations that are non-conservative

and that result in no change of affinity are not contact residues. The mutations at contact residues that result in no change of affinity are very conservative mutations. The crystal structure shows only three other residues, H35N, H105A and H106M that participate in binding (mostly to lactone) that are not predicted by the computer model binding site and were not mutated.

The mechanism of digoxin binding to the other monoclonal anti-digoxin antibodies is not yet known. Preliminary experiments measuring specificity of at least one other anti-digoxin antibody, 40-100, show significant, but relatively less ability of this antibody, as compared with 26-10, to distinguish dihydrodigoxigenin from digoxin (Near, unpublished experiments). This suggests that 40-100 has a weaker, but still significant, interaction with the lactone ring (Near, unpublished). Antibody 40-100 is, however, highly affected by substitutions on the steroid nucleus and by removal of the sugar moieties (Mudgett-Hunter *et al.*, 1985; Near, 1990 and unpublished data). The binding properties of 40-100 would be consistent with a binding site composed of a slot into which digoxin would fit lengthwise, without lactone as the dominant moiety for determining overall binding strength. This antibody shares great L chain homology with 26-10 (only differing at eight amino acids, three of which are in CDR segments at L39, L96 and L101) (Hudson *et al.*, 1990). Therefore, we hypothesize that L chain positions L39, L96 and L101 are important in determining the shape and interactions of the binding site, especially in the area where lactone binding is involved. Preliminary mutagenesis at these positions in the context of both the 26-10 and 40-100 H chains (by transfection experiments) strongly support this (Near, unpublished experiments). A different antibody, 40-120, behaves more like 26-10, with the specificity of dihydrodigoxigenin relative to digoxin showing about 1500-fold lower binding, but it is more affected by steroid substitutions and loss of sugars than is 26-10 (Mudgett-Hunter *et al.*, 1985; Near *et al.*, 1991; Near, unpublished experiments). The 40-120 binding site could be intermediate between that of 26-10 and 40-100, involving a deeper slanted slot or a slanted pocket. The contribution of lactone to the binding of the other available monoclonal antibodies has not been investigated, but the specificity results indicate that there may be four or five different kinds of digoxin binding sites (Mudgett-Hunter *et al.*, 1985; Near *et al.*, 1991; Near, unpublished). These observations would not be consistent with lactone being an "immunodominant" portion of digoxin in terms of producing large populations of antibodies that interact most strongly with the lactone moiety of digoxin.

Acknowledgements—We thank Boutrous Bouyounes, Cynthia Mallion, Abbie White and Mary Ann Wright for their technical assistance. We also thank Amy Lister for helping to edit this manuscript. Phil Jeffrey and Steve Sheriff were kind enough to share data on the crystal structure of the 26-10 antibody. We also thank Dr Edgar Haber for his support and interest in this project.

REFERENCES

Bates R. M., Ballard D. W. and Voss E. W. (1985) Comparative properties of monoclonal antibodies comprising a high-affinity anti-fluorescyl idiotype family. *Molec. Immun.* **22**, 871–877.

Bedzyk W. K., Johnson L. S., Riordan G. S. and Voss Jr. E. W. (1989) Comparison of variable region primary structures within an anti-fluorescein idiotype family. *J. biol. Chem.* **264**, 1565–1569.

Bruccoleri R. and Karplus M. (1987) Prediction of the folding of short polypeptide segments by uniform conformational sampling. *Biopolymers* **26**, 137–144.

Bruccoleri R., Haber E. and Novotny J. (1988) Structure of antibody hypervariable loops reproduced by a conformational search algorithm. *Nature* **335**, 564–567 [Erratum (1988) *Nature* **336**, 266].

Brunger A. T. (1991) Solution of a Fab (26-10)/digoxin complex by generalized molecular replacement. *Acta Cryst.* **A47**, 195–204.

Chothia C. (1974) Hydrophobic binding and accessible surface area in proteins. *Nature* **248**, 338–339.

Fieser L. G. and Fieser M. (1959) *Steroids* (Edited by Fieser L. G. and Fieser M.) p. 727. Reinhold, New York.

Go K., Kartha G. and Chen J. P. (1980) The structure of digoxin. *Acta Cryst.* **B36**, 1811–1816.

Herron J. N., He X., Mason M. L., Voss Jr. E. W. and Edmundson A. B. (1989) Three-dimensional structure of a fluorescein–Fab complex crystallized in 2-methyl-2,4-pentanediol. *Proteins* **5**, 271–280.

Hudson N. W., Bruccoleri R. E., Steinrauf L. K., Hamilton J. A., Mudgett-Hunter M. and Margolies M. N. (1990) A Vk–Jk junctional change in an antidigoxin recombinant antibody destroys digoxin binding activity. *J. Immun.* **145**, 2718–2725.

Kabat E. A. (1966) The nature of an antigenic determinant. *J. Immun.* **97**, 1–11.

Kunkel T. A. (1985) Rapid and efficient site-specific mutagenesis without phenotypic selection. *Proc. natn. Acad. Sci. U.S.A.* **82**, 488–493.

Mudgett-Hunter M., Anderson W., Haber E. and Margolies M. N. (1985) Binding and structural diversity among high-affinity monoclonal anti-digoxin antibodies. *Molec. Immun.* **22**, 477–488.

Mudgett-Hunter M., Margolies M. N., Ju A. and Haber E. (1982) High affinity monoclonal antibodies to the cardiac glycoside digoxin. *J. Immun.* **129**, 1165–1172.

Mulligan R. C. and Berg P. (1980) Expression of a bacterial gene in mammalian cells. *Science* **209**, 1422–1427.

Munson P. J. and Robard D. (1980) LIGAND: a versatile computerized approach for characterization of ligand-binding systems. *Analyt. Biochem.* **107**, 220–227.

Near R. I. (1992) Gene conversion of immunoglobulin variable regions in mutagenesis cassettes by replacement PCR mutagenesis. *BioTechniques* **12**, No. 1, 88–97.

Near R. I., Bruccoleri R., Novotny J., Hudson N. W., White A. and Mudgett-Hunter M. (1991) The specificity properties that distinguish members of a set of homologous anti-digoxin antibodies are controlled by H chain mutations. *J. Immun.* **146**, 627–633.

Near R. I. and Haber E. (1989) Characterization of the heavy and light chain immunoglobulin variable region genes used in a set of anti-digoxin antibodies. *Molec. Immun.* **26**, 371–382.

Near R. I., Ng S. C., Mudgett-Hunter M., Hudson N. W., Margolies M. N., Seidman J. G., Haber E. and Jacobson

M. A. (1990) Heavy and light chain contributions to antigen binding in an anti-digoxin chain recombinant antibody produced by transfection of cloned anti-digoxin antibody genes. *Molec. Immun.* 27, 901–909.

Novotny J., Bruccoleri R. E. and Saul F. A. (1989) On the attribution of binding energy in antigen–antibody complexes McPC603, D1.3 and HyHEL-5. *Biochemistry* 28, 4735–4749.

Panka D. J. and Margolies M. N. (1987) Complete variable region sequences of five homologous high affinity anti-digoxin antibodies. *J. Immun.* 139, 2385–2391.

Rose D. R., Strong R. K., Margolies M. N., Gefter M. L. and Petsko G. A. (1990) Crystal structure of the antigen-binding fragment of the murine anti-arsonate monoclonal antibody 36-71 at 2.9 Å resolution. *Proc. natn. Acad. Sci. U.S.A.* 87, 338–342.

Sanger F. S., Nicklen S. and Coulson A. R. (1977) DNA sequencing with chain-terminating inhibitors. *Proc. natn. Acad. Sci. U.S.A.* 74, 5463–5468.

Satow Y., Cohen G. H., Padlan A. and Davies D. R. (1986) Phosphocholine binding immunoglobulin Fab McPC603: An x-ray diffraction study at 2.7 Å. *J. molec. Biol.* 190, 593–604.

Schildbach J. F., Panka D., Parks D. R., Jager G. C., Novotny J., Herzenberg L. A., Mudgett-Hunter, M., Bruccoleri R. E., Haber E. and Margolies M. N. (1991) Altered hapten recognition by two anti-digoxin hybridoma variants due to variable region point mutations. *J. biol. Chem.* 266, 4640–4647.

Southern P. J. and Berg P. (1982) Transformation of mammalian cells to antibiotic resistance with a bacterial gene under control of the SV40 early region promoter. *J. molec. Appl. Genet.* 1, 327–341.

Strong R. K., Petsko G. A., Sharon J. and Margolies M. N. (1991) Three-dimensional structure of murine anti-azophenylarsonate Fab 36-71: 2. Structural basis of hapten binding and idiotypy. *Biochemistry* 30, 3749–3757.

ANALYTICAL BIOCHEMISTRY 229, 282–290 (1995)

Codon-Based Combinatorial Alanine Scanning Site-Directed Mutagenesis: Design, Implementation, and Polymerase Chain Reaction Screening

Jean Chatellier,* Alberto Mazza,† Roland Brousseau,† and Thierry Vernet†,[1]

Laboratoire d' Immunochimie, Institut de Biologie Moléculaire et Cellulaire du CNRS, 15 rue R. Descartes, 67084 Strasbourg Cédex, France; and †Biotechnology Research Institute of NRC, 6100 avenue Royalmount, Montréal, Québec, Canada H4P 2R2

Received April 7, 1995

Combinatorial alanine scanning mutagenesis is a powerful tool for the exploration of protein structure–function relationships. Unfortunately, combinatorial alanine replacement of multiple residues using standard site-directed mutagenesis is restricted to a subset of amino acids. To circumvent this limitation, an efficient procedure for combinatorial site-specific replacement by alanine of any residue in a given protein sequence has been established. The method, which involves simple procedures and commonly used materials, is based upon the use of codon-based mutagenesis. A defined ratio of alanine to wild-type codon was introduced at each predetermined triplet using the "column-splitting" technique during oligonucleotide synthesis. High-throughput genetic screening of mutant libraries was facilitated by the incorporation of diagnostic restriction sites at targeted codons followed by a PCR-based screening procedure. The method was tested on a set of 13 residues located at the interface between the variable domains of a Fab fragment of an antibody. The occurrence of alanine substitutions was found to be comparable to the statistically predicted distribution.

Site-directed mutagenesis has proven to be an invaluable tool for the analysis of protein structure–function relationships. A variety of strategies have been developed to mutate a specific amino acid or group of residues at predetermined sites in protein sequences (1,2). The importance of amino acid side chains on specific protein functions has often been established by alanine scanning mutagenesis where targeted residues are systematically replaced by alanine (3). Indeed, incorporation of the chemically simple methyl group of alanine eliminates a residue's side chain, while limiting structural perturbations due to steric hindrance effects (4,5).

Sequential replacement by alanine has been used to explore protein-interacting surfaces (6), protein–DNA binding activity (7), and the mechanism of enzymes (8,9). As an extension of sequential alanine scanning, multiple replacement of sets of residues by alanine is a powerful way to probe subtle relationships between residues in proteins (10). For such purpose, the combinatorial mutagenesis technique provides an efficient way to investigate the effects of a given mutation in the context of other mutations (11,12).

To study the role of framework residues located at the interface between the variable domains of the heavy (VH) and light (VL) chains of an Fab,[2] we considered the consequences of their combinatorial replacement by alanine. This approach required (i) the replacement of each targeted sites by alanine excluding any other side chains, (ii) a given probability of alanine substitution at each targeted site, and (iii) alanine replacement at targeted sites independent from each other. Unfortunately, combinatorial replacement of multiple amino acids by alanine using standard site-directed mutagenesis of individual nucleotides is restricted to seven amino acids (Asp, Glu, Gly, Pro, Ser, Thr, and Val) (11). Moreover, multiple nucleotide replacements by *in vitro* saturation mutagenesis would result in the incorporation of side chains other than alanine (13–15).

[1] To whom correspondence should be addressed at present address: Institut de Biologie Structurale, 41 avenue des Martyrs, 38027 Grenoble Cédex 1, France. Fax: (33) 76.88.54.94. E-mail: vernet@ibs.fr.

[2] Abbreviations used: Fab, antibody fragment; oligo, oligonucleotide; ssDNA, single-stranded DNA.

0003-2697/95 $12.00

To circumvent the limitations of previous methods, we applied a codon-based mutagenesis approach to combinatorial alanine scanning mutagenesis. Codon-based mutagenesis allows the selective substitution of any target amino acid since entire nucleotide triplets are replaced. The probability of amino acid replacement at predefined sites depends upon the ratio of mutant to wild-type codon incorporated during the oligo synthesis. Two different strategies have been published for codon-based mutagenesis using synthetic oligos. The first strategy is based upon the incorporation of preexisting triplets of nucleotides during oligo synthesis. However, the synthesis yield reported to date is still too low for applications requiring large oligos, i.e., oligos incorporating multiple mutagenic codons (16). The second approach, the column-splitting synthesis technique, relies upon standard synthetic DNA chemistry. The incorporation of entire codons at mutation sites is performed on two separate columns (17–19). The mutation frequency is controlled by the ratio of solid support split between the mutant and the wild-type columns.

In this paper we have applied the codon-based mutagenesis procedure using synthetic oligos obtained by the column-splitting technique to combinatorial alanine scanning mutagenesis. The method was tested on a set of residues of Fab 57P (unpublished results). The resulting libraries of *Escherichia coli* clones have been screened using a rapid PCR-based strategy. The procedure has provided an efficient way of generating representative repertoires of mutants among which distribution of multiple mutants can be predicted using a statistical procedure.

MATERIALS AND METHODS

Construction of Plasmid pJC 57P

DNA manipulations and analysis were carried out essentially using standard protocols (20). Restriction endonucleases and DNA-modifying enzymes were purchased from Bethesda Research Laboratories, Boehringer–Mannheim, New England Biolabs, and Pharmacia LKB Biotechnology Inc. The expression plasmid pJC 57P used in this study (Fig. 1A) derives from phagemid pHL 57P which encodes the heavy truncated Fd (VH-CH1) and the light κ (VL-Cκ) regions of Fab 57P fragment (unpublished results). pJC 57P was constructed by replacing the 51-base pairs (bp) *SpeI/Eco*RI DNA fragment of pHL 57P with a synthetic DNA cassette consisting of two oligos, 5′-CTAGTGAACAAA-AACTGATATCAGAAGAGGATCTG**AGATCT**CATC-ACCATCACCATCACTAATAGG-3′ and 5′-AATTCCT-ATTAGTGATGGTGATGGTGATGAGACTCAGATC-CTCTTCTGATATCAGTTTTTGTTAC-3′. The cassette encodes a 10-amino acid peptide of the human c-myc protein (21) fused via a 2-amino acid spacer with six histidine residues (22) and creates a recognition site for the restriction enzymes *Eco*RV (underlined) and *Bgl*II (bold characters). Both *Spe*I and *Eco*RI cloning sites were regenerated by the insertion of the synthetic DNA cassette. Plasmid modification was verified by restriction enzyme mapping and by DNA sequencing using the T7 DNA polymerase (Pharmacia LKB Biotechnology Inc.) and primer 5′-CAGCTCAGTGACTGTCC-3′.

Selection of Fab 57P Residues for Mutagenesis

Residues that are likely to be in contact across the interface between the VH and the VL domains of Fab 57P were identified by an analysis of conserved interdomain contacts in IgG Fabs of known crystallographic structure (unpublished results). Seven VH and six VL residues of Fab 57P were selected for mutagenesis.

Synthesis of Oligodeoxyribonucleotides

All oligos were synthesized using standard cyanoethyl phosphoramidite chemistry on an Applied Biosystems Model 394 DNA synthesizer. As an example, the synthesis scheme for the mutagenic oligo JCo4 is illustrated in Fig. 2. At the targeted codon, the column was dismantled and the solid support was split into two portions that were repacked into two columns designated as the mutant and the wild-type columns corresponding to 25 and 75% of the initial volume of resin, respectively. The next three synthesis cycles allowed for the incorporation of an alanine codon in the former column and of the wild-type codon in the latter column. The contents of the two columns were then combined together and the oligos extended to the next targeted site where the column was split again. The synthesis results in a population of mutagenic oligonucleotides that will be hereafter referred to as mutagenic oligos.

The scale of the synthesis for the mutagenic oligos was increased from the usual amount of 40 nmol to 80 nmol to compensate for the inevitable handling losses involved in splitting and reuniting the column contents. Before each transfer, the synthesis solid support (polystyrene based; Applied Biosystems) was dried for 5 min using a gentle flow of nitrogen gas while still in the synthesis column(s). The splitting was performed on a volumetric basis by pouring the dried solid support into a narrow plastic tube, tapping the tube on a solid surface to ensure even packing, and measuring off one-quarter of the length of the tube. This procedure avoided weighing the very light, electrostatic polystyrene solid support powder, thus reducing losses. A larger than usual excess of reagents was used, i.e., the synthesis was run with the 200 nmol synthesis cycle to ensure a better yield.

To prevent bias against mutated triplets in the 5′ portion of the oligos due to products of lower chain length in the resulting oligo populations, the mutagenic

oligos were purified by 15% polyacrylamide/8 M urea PAGE followed by a Sep Pak C18 column (Waters Associates) as previously described (23). Oligo primers for PCR and DNA sequencing were purified by chromatography on a Sep Pak C18 column. The oligo concentrations were determined by absorbance readings at 260 nm.

In Vitro Site-Directed Mutagenesis

The reagents used for mutagenesis were purchased from Bio-Rad and Pharmacia LKB Biotechnology Inc. *In vitro* site-directed mutagenesis (24) reactions were performed using uracil-containing ssDNA (25) obtained by infection with the helper phage M13KO7 (26) of *E. coli* strain CJ236 (Bio-Rad) harboring pJC 57P. The four mutagenic oligonucleotides used in this study are depicted in Fig. 1B. The four single-oligo mutant libraries, hereafter referred to JCo1, JCo2, JCo3, and JCo4 libraries, were constructed using one mutagenic oligo (Figs. 1A and 1B). An equimolar mixture of two mutagenic oligos was used to create two double-oligo mutant libraries, hereafter referred to JCo1 + JCo2 and JCo3 + JCo4 libraries (Figs. 1A and 1B). Two picomoles of mutagenic oligo phosphorylated at the 5′ terminus using T4 polynucleotide kinase (New England Biolabs) was annealed to 0.2 pmol of the ssDNA template in a final volume of 20 μl of 20 mM Tris–HCl, pH 7.4, 2 mM $MgCl_2$, and 50 mM NaCl by incubating at 70°C for 5 min, at 56°C for 20 min, at 37°C for 20 min, and on ice for a minimum of 5 min. Two microliters of 250 mM Tris–HCl, pH 8.0, 50 mM $MgCl_2$, 350 mM NaCl, 15 mM dithiothreitol, 7.5 mM ATP, and 4 mM each of dATP, dCTP, dGTP, and dTTP was then added to 10 μl of the annealing mixture. Complementary strand DNA synthesis was performed in the presence of 3 units of T4 DNA polymerase, 3.5 units of T4 DNA ligase, and 1 unit of T4 protein gene 32 by incubation on ice for 5 min, at room temperature for 5 min, and at 37°C for 90 min. The reaction was stopped by heating to 65°C for 20 min.

Preparation of *E. coli* competent cells and transformation reactions were performed as previously described (27). One-half of the final volume of the *in vitro* mutagenesis mixtures was used to transform 150 μl of competent BMH 71-18 *E. coli* (*dut*$^+$, *ung*$^+$) cells (28). pJC 57P supercoiled DNA (100 ng) was transformed in parallel as control. Transformants were isolated onto ampicillin-selective LB–agar medium (20).

Library Screening by PCR and Restriction Analysis

Individual bacterial transformants were transferred with a sterile toothpick into a PCR mixture consisting of 75 pmol of each primer in 60 μM dNTPs, 10 mM Tris–HCl, pH 8.3, 1.5 mM $MgCl_2$, and 50 mM KCl and 2 units of *Taq* DNA polymerase (Boehringer–Mannheim) for a final volume of 75 μl. The mixture was then incubated for 3 min at 94°C to lyse the cells and subjected to 25 thermocycles of amplification (29) in a TwinBlock System (Easy-Cycler Series, Ericomp Inc.) as follows: 1 min at 94°C to denature the template DNA, 1 min at 62°C for primer annealing, and 2 min at 72°C for DNA extension. PCR synthesis of H chain libraries was achieved using H*for* primer 5′-GGTGAAACTGCTCGAGTCTGG-3′ in combination with H*rev* primer 5′-CAGTTTTTGTTCACTAGTACAATCC-3′ (Fig. 1B). These primers contain an *Xho*I and *Spe*I restriction site (underlined), respectively. The L chain libraries were amplified using L*for* primer 5′-CCATGGCCGAGCTCGTGATGACC-3′ with L*rev* primer 5′-GCTTAACTCTAGAATTAACACTCATTCC-3′ (Fig. 1A). These primers contain an *Sac*I and *Xba*I restriction site (underlined), respectively.

A 10-μl aliquot of the PCR reactions was incubated for 2 h at optimal temperature in 96-well plates (Nunc) with 2.5 units of the appropriate restriction enzymes in a final volume of 30 μl of the reaction buffer supplied by the manufacturers and analyzed by agarose gel electrophoresis (20). The regions surrounding the mutagenic windows were sequenced (30) to ensure that no alterations other than the desired mutations were introduced into the target sequences. The sequence of mutants resulting from H chain libraries was obtained with primers 5′ VH 5′-GAGCTGATGAAGCCTGG-3′ and/or 3′ VH 5′-GCCAGTGGATAGACAGATGG-3′ derived from sequences 5′ and 3′ to the Fd coding region, respectively. Mutants arising from L chain libraries were sequenced using primers 5′ VL 5′-CTCGTGATGACCCAGAC-3′ and/or 3′ VL 5′-GCACACGACTGAGGCAC-3′ derived from sequences 5′ and 3′ to the κ coding region, respectively.

Mutation Frequency and Library Size

The probability F_i of occurrence of i multiple mutants is given by the classical binomial distribution

$$F_i = [n!/i!(n - i)!]p^i(1 - p)^{n-i}, \qquad [1]$$

where n is the total number of targeted sites and p is the ratio of alanine to wild-type codon at each targeted triplet. The calculation is based on the assumption that each site is mutated independently from other sites with an equal probability p of mutation. This will be verified if (i) the solid support is accurately split during synthesis, i.e., alanine replacement occurs at a predetermined ratio; (ii) alanine codons are equally incorpo-

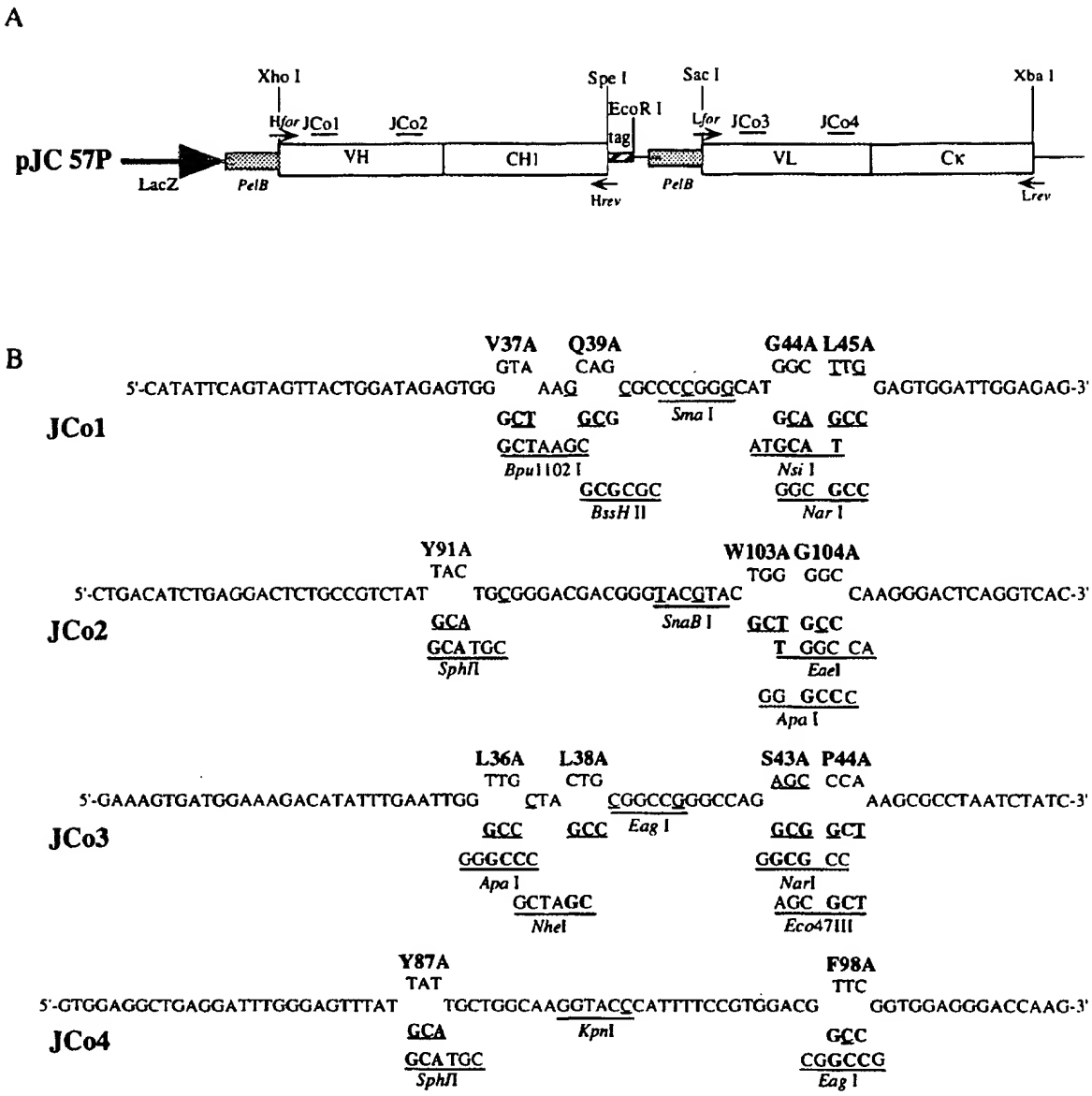

FIG. 1. (A) Schematic location of mutagenic oligos and PCR primers relative to pJC 57P template. Synthetic mutagenic oligos and PCR primers are indicated by dashes and arrows, respectively. Unique restriction sites are indicated. *LacZ*, β-galactosidase promoter; *PelB*, signal peptide sequence of bacterial pectate lyase (32); VH-CH1 and VL-Cκ, Fd heavy and κ light coding regions of Fab 57P, respectively; tag, c-myc peptide and (His6) immunodetection and purification tag, respectively. (B) Design of mutagenic oligos used in this study. The denomination of the mutagenic oligos is given in the left margin. The numbering of amino acid residues follows the convention of Kabat *et al.* (33). Each targeted amino acid is referred to by the nature and position of the change (e.g., V37A referring to the substitution of Val 37 by Ala). Silent diagnostic restriction sites involving alanine codons (bold characters) generated by the mutagenesis are indicated below the corresponding targeted positions. The centrally located restriction sites diagnostic of mutagenesis efficiency are shown. The mismatches leading to the creation of endonuclease recognition sequences are underlined.

rated at each mutated position; (iii) the efficiency of *in vitro* mutation is equivalent for all oligos present in the final population; and (iv) plasmids are transformed and propagated with equal efficiency in *E. coli* host cells.

The minimum number N of individual colonies re-

quired for screening to obtain all possible combinations of alanine replacement with a high degree of certainty is given by

$$N = [1/(F(1/M))]\ln[1/(1 - A)], \quad [2]$$

where F is the frequency of occurrence of the mutation corresponding to all targeted sites of the library substituted by alanine, M is the efficiency of mutagenesis, and A is the degree of certainty.

RESULTS AND DISCUSSION

Mutagenic Oligonucleotide Design and Synthesis

The 13 residues at the VH–VL interface of Fab 57P selected for alanine replacement mutagenesis define four different clusters each of a size compatible with oligo synthesis. The four mutagenic oligos include features designed to improve the efficiency of *in vitro* mutagenesis and to facilitate the screening of mutant libraries (Fig. 1B). First, to reduce strand displacement during enzymatic extension and ligation, the 5′ sequence upstream of the first mutagenic site was lengthened to 27 nucleotides against 15 bases at the 3′ end. Second, each mutagenic oligo contains different silent restriction endonuclease cleavage sites: (i) one centrally located for the evaluation of *in vitro* mutagenesis efficiency and (ii) one at each mutated position to facilitate the screening of mutant libraries, taking advantage of the fact that all four alanine codons are found in highly expressed *E. coli* genes (31). Most of the silent diagnostic sites were chosen to be unique within the PCR-amplified fragment used for diagnostic purposes. This approach is applicable to virtually any target DNA sequence, since restriction sites involving alanine codons recognized by commercially available enzymes are numerous (Table 1).

A population of oligos harboring at each selected position either alanine or the wild-type codon in a predefined ratio was synthesized by the column-splitting technique (17–19). The frequency of alanine replacement at each targeted site is controlled by the ratio of solid support split between the mutant and the wild-type columns. The expected frequency of occurrence of each oligo present in the final population (Fig. 2) can be calculated from this ratio using Eq. [1] (Materials and Methods). A ratio of alanine to wild-type codon of 25% was chosen to provide a balanced distribution between the restoration of wild-type sequences ($i = 0$, Eq. [1]) and the generation of single or multiple alanine mutants ($i > 0$). As the total number of mutant sites increases, the proportion of wild-type sequences will drop. For instance, with 7 target positions, the JCo1 + JCo2 library has a 0.13 theoretical frequency of wild-type sequences, whereas this proportion will be 0.02 for all 13 targeted site libraries.

TABLE 1

Restriction Sites (Six Bases) Available Containing Alanine Codons

1. GCNNNN	
*Sph*I	GCATG/C
*Nae*I	GCC/GGC
*Bss*HII	G/CGCGC
*Nhe*I	G/CTAGC
2. NGCNNN	
*Eco*47III	AGC/GCT
*Nar*I	GG/CGCC
*Fsp*I	TGC/GCA
3. NNGCNN	
*Pst*I	CTGCA/G
*Apa*LI	G/TGCAC
*Nsi*I	ATGCA/T
*Eae*I	Y/GGCCR (Y = C or T; R = A or G)
*Eag*I	C/GGCCG
*Stu*I	AGG/CCT
*Apa*I	GGGCC/C
*Msc*I	TGG/CCA
*Mlu*I	A/CGCGT
*Sac*II	CCGC/GG
*Bss*HII	G/CGCGC
*Nru*I	TCG/CGA
*Hind*III	A/AGCTT
*Pvu*II	CAG/CTG
*Sac*I	GAGCT/C
4. NNNGCN	
*Fsp*I	TGC/GCA
*Nar*I	GG/CGCC
*Eco*47III	AGC/GCT
5. NNNNGC	
*Nhe*I	G/CTAGC
*Bss*HII	G/CGCGC
*Sph*I	GCATG/C
*Nae*I	GCC/GGC

Note. The nucleotides in the recognition sequence that correspond to the alanine codons are shown in bold characters. N represents any of the four bases.

Construction and PCR-Based Screening of Mutant Libraries

One single mutagenic oligo was used to modify by *in vitro* mutagenesis various target amino acid positions close in the primary sequence of the protein, reducing efforts in the mutagenesis experiment and cost for DNA synthesis. Positions that are remote from each other were mutated by a mixture of different single mutagenic oligos (Figs. 1A and 1B). The number of mutated positions can also be modulated by recombining various libraries using the unique cloning sites of the H and L chains (Fig. 1A). About 2×10^4 BMH 71-18 transformants were obtained for the four single-oligo and the two double-oligo libraries. Between 5 and 10 transformants were observed in the absence of primer, indicating that the template itself contributes minimally to the background.

Transformants were tested by restriction analysis of PCR-amplified DNA fragments. The yield of incorporation of mutagenic oligos was first determined using the centrally located diagnostic restriction site (Fig. 1B), indicating the efficiency of mutagenesis. In a second step, individual alanine replacements were identified by their corresponding restriction diagnostic sites (Fig. 1B). As an example, the restriction patterns of PCR products from three different clones (a, b, and c) arising from JCo1 library analyzed by gel electrophoresis are given in Fig. 3. The incorporation of JCo1 mutagenic oligo in all three clones is demonstrated by the shift in size compared to the control after digestion by *Sma*I (Fig. 3, lanes 3–6). The various patterns of fragments clearly indicate the presence or the absence of an ala-

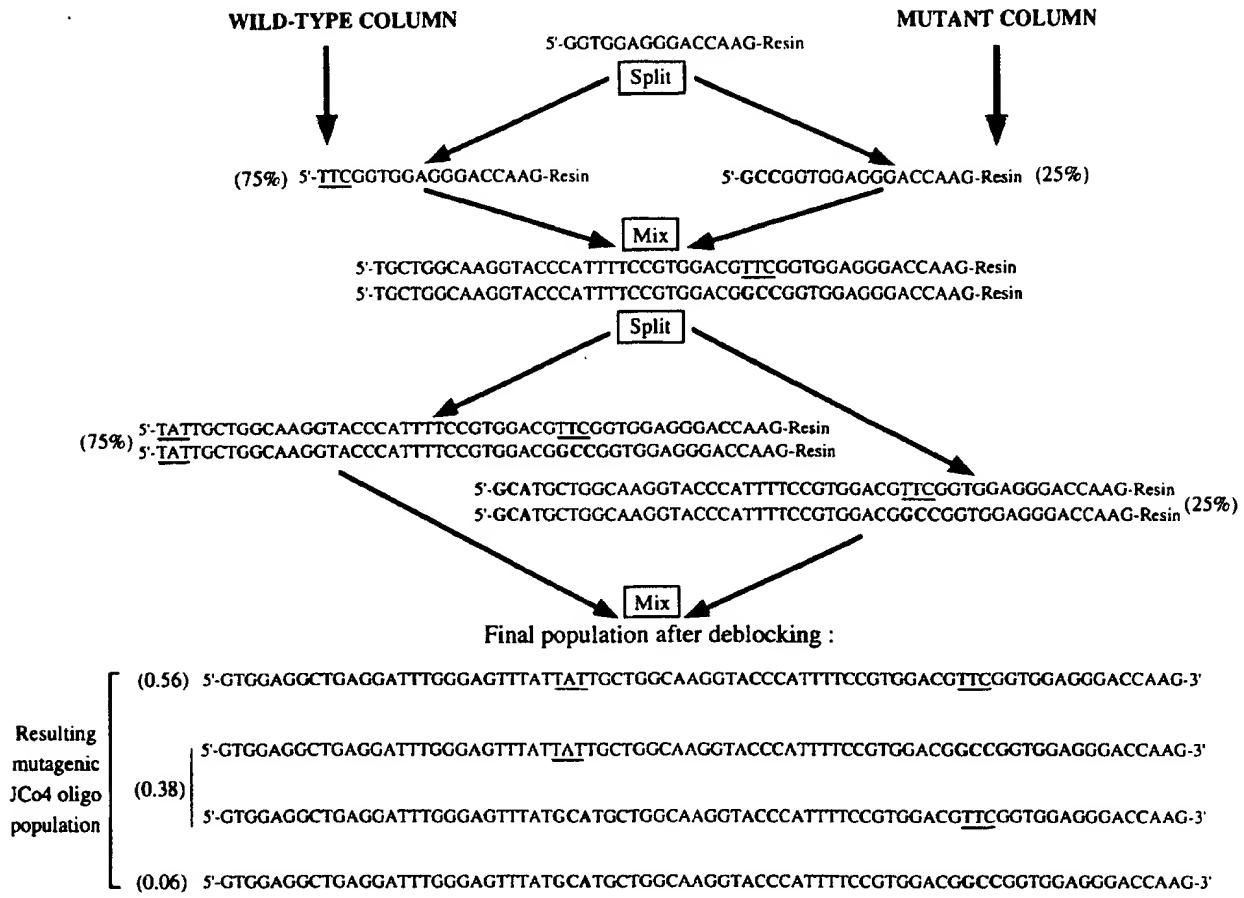

FIG. 2. Synthesis of mutagenic oligos using the column-splitting technique. The synthesis of JCo4 mutagenic oligo (Fig. 1B) is given as an example. At a codon-targeted position, the column was dismantled and the solid support was split into two portions (%) that were repacked into the mutant and the wild-type columns. On the mutant column, three rounds of synthesis were performed with nucleotide precursors of alanine codon (bold characters), whereas the wild-type column was subjected to three synthetic cycles with the wild-type nucleotide precursors (underlined). After synthesis of each codon the two columns were combined together, and the process was repeated for the subsequent codon to be mutated. Expected frequency (see Eq. [1]; Materials and Methods) of each mutagenic oligo in the final population is given (within parentheses) to the left of the sequences.

nine at a given site. Clone a possesses an alanine at position 37 (digested by *Bpu*1102 I; Fig. 3A, lane 10) and at position 45 (digested by *Nar*I; Fig. 3B, lane 10) but has wild-type amino acids at positions 39 and 44 as revealed by the absence of *Bss*HII (Fig. 3B, lane 2) and *Nsi* I (Fig. 3B, lane 5) restriction sites, respectively. A similar analysis shows that residues Gln39 and Leu45 of clone b are substituted by alanine and that clone c is mutated at positions 39 and 44. However, double mutations at consecutive targeted sites cannot be identified unambiguously, due to the overlap of restriction site sequences. As an example, the Gln44Ala-Leu45Ala double mutant does not contain *Nsi* I or *Nar*I diagnostic sites (Fig. 1B). These ambiguities were removed by systematic DNA sequencing of negative clones for consecutive mutation sites.

Mutation Frequency and Distribution

Approximately 100 clones randomly selected in each library were screened by the PCR-based procedure. As shown in Fig. 4, the efficiency of *in vitro* mutagenesis in the four single-oligo libraries ranges from 58 to 84%. These values are comparable to those previously reported for single-base substitutions (25). This yield decreases when the total number of target positions increases, presumably due to the higher number of nucleotide mismatches involved. In JCo1 + JCo2 and JCo3 + JCo4 double-oligo libraries, the efficiency of double mutagenesis was lower (21 and 50%, respectively), with a three times higher incorporation efficiency of the oligo at the 3′ end of the pair compared to that at the 5′ end.

The observed occurrence of mutant combinations for the four single-oligo libraries is given in Table 2. Each targeted site was found to be mutated. Multiple mutants with a low probability of occurrence were not observed because of the limited number of clones analyzed. The frequency of alanine to wild-type amino acid replacement at each targeted site calculated from these data (Fig. 4) ranges from 10 to 29%, encompassing the 25% expected frequency. The average frequency over the 13 sites is 19%. These values are not correlated with the number of mismatches at a given position. For instance, with two mismatches, position 44 of oligo JCo3 is replaced in only 10% of the clones, whereas position 103 of oligo JCo2 with three mismatches is replaced in 26% of the clones tested (Figs. 1B and Fig. 4). Neither the number of mutation sites nor their position within the mutagenic oligos had an obvious influence on the level of alanine substitution. The reasons why the efficiency of alanine replacement varies remain unclear and may be related either to bias during the oligo synthesis and/or to variation in the efficiency of incorporation of each oligo present in the final population during the *in vitro* mutagenesis. Alternatively, some mutants may be selected against in *E. coli*.

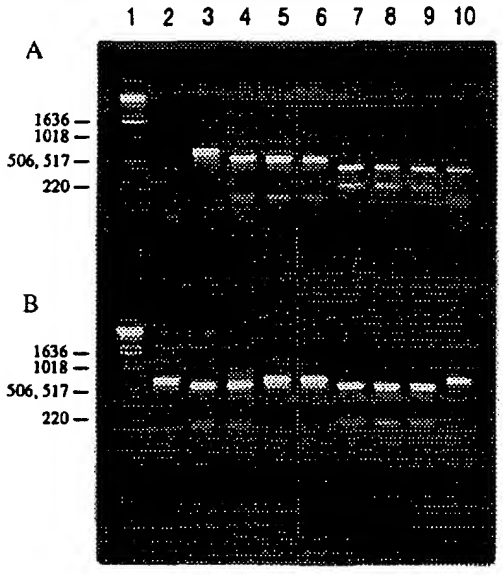

FIG. 3. PCR-based colony-screening procedure. Ethidium bromide-stained agarose (1.5%) gel electrophoresis of restriction digests of PCR products. PCR-based analysis of three different clones (a, b, and c) from JCo1 library (Fig. 1) as an example is shown. Amplification was performed using primers H*for* and H*rev* (Materials and Methods) and the resulting PCR products were digested with the appropriate restriction enzymes prior to electrophoresis. (A) PCR reaction with a control *E. coli* BMH 71-18 clone (lane 2); *Sma*I digests (lanes 3–6); *Bpu*1102I digests (lanes 7–10); digestion analysis of the control fragment obtained by PCR amplification of *E. coli* BMH 71-18 clone harboring pJC 57P plasmid (lanes 3 and 7); digestion analysis of clones a (lanes 4 and 10), b (lanes 5 and 9), and c (lanes 6 and 8). (B) *Bss*HII digest (lanes 2–4); *Nsi*I digests (lanes 5–7); *Nar*I digests (lanes 8–10); digestion analysis of clones a (lanes 2, 5, and 8), b (lanes 3, 6, and 9), and c (lanes 4, 7, and 10). The size reduction of the DNA fragment following digestion is diagnostic for alanine substitution at the target position. DNA molecular weight markers are 1-kb ladders (BRL; lane 1). The sizes of marker DNA fragments are listed in the left margin.

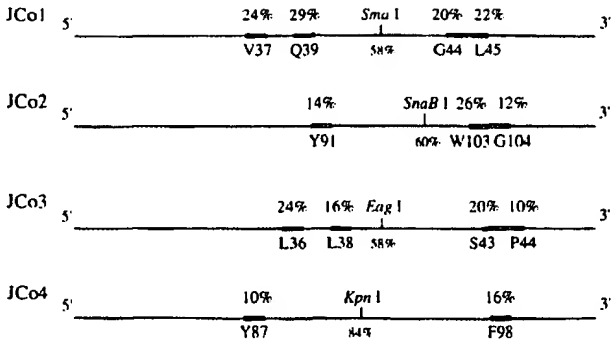

FIG. 4. Experimental frequencies of *in vitro* mutagenesis. Libraries are listed in the left margin. The percentage of mutagenic oligo incorporation was determined from approximately 100 clones randomly selected in each library and screened by the PCR-based procedure. The efficiency of mutagenesis is indicated below the centrally located restriction site. The yields of alanine incorporation derived from data presented in Table 2 are given above the corresponding targeted positions.

Theoretical and experimental distributions of the occurrence of multiple mutants are compared in Table 3. As expected, the best match between theoretical and experimental values is obtained for libraries with an observed alanine replacement frequency at each target site close to the expected frequency of 25% (Fig. 4 and Table 3, compare JCo1 and JCo3). Deduced from data in Fig. 4, the experimental frequency of alanine replacement at each site departs from the expected frequency with average values of 0.24, 0.17, 0.18, and 0.13 for JCo1, JCo2, JCo3, and JCo4, respectively. These average values were used as an approximation of p to recalculate the theoretical distributions of multiple mutants using Eq. [1]. The theoretical distributions using these corrected values for p are closer to the observed distributions (Table 3).

Concluding Remarks

(i) The codon-based mutagenesis approach is a general method to introduce any selected residue, deletion, or insertion in a given protein sequence. We have shown that representative repertoires of alanine mutants can be constructed using oligonucleotides synthesized by the column-splitting technique and that the probability of multiple mutant occurrence corresponds to the statistically expected value. The possibility of

TABLE 2

Occurrence of Observed Mutants for the Four Single-Oligo Libraries[a]

Mutant	Number of isolates	Mutant	Number of isolates
JCo1 library		JCo3 library	
Wild-type	20	Wild-type	27
V37A	4	L36A	7
Q39A	6	L38A	2
G44A	3	S43A	4
L45A	3	P44A	2
V37A-Q39A	1	L36A-L38A	3
V37A-G44A	2	L36A-S43A	2
V37A-L45A	3	L36A-P44A	0
G44A-L45A	0	S43A-P44A	1
Q39A-G44A	3	L38A-S43A	1
Q39A-L45A	4	L38A-P44A	0
V37A-Q39A-G44A	1	L36A-L38A-S43A	0
V37A-Q39A-L45A	0	L36A-L38A-P44A	0
Q39A-G44A-L45A	0	L38A-S43A-P44A	2
V37A-G44A-L45A	1	L36A-S43A-P44A	0
V37A-Q39A-G44A-L45A	0	L36A-L38A-S43A-P44A	0
JCo2 library		JCo4 library	
Wild-type	29	Wild-type	36
Y91A	2	Y87A	5
W103A	10	F98A	8
G104A	4	Y87A-F98A	0
Y91A-W103A	3		
Y91A-G103A	2		
W103A-G104A	0		
Y91A-W103A-G104A	0		

[a] The background of clones lacking the incorporation of the mutagenic oligo was not considered for analysis.

TABLE 3

Comparison of Observed[a] and Calculated Frequencies of Multiple Mutations for Each Single-Oligo Library

i[b]	0	1	2	3	4
JCo1	0.39	0.31	0.25	0.04	0
(n = 4)[b]	(0.32)[c]	(0.42)	(0.21)	(0.05)	(0.004)
p = 0.24[d]	[0.33][e]	[0.42]	[0.20]	[0.04]	[0.003]
JCo2	0.58	0.32	0.10	0	
(n = 3)	(0.42)	(0.42)	(0.14)	(0.02)	
p = 0.17	[0.57]	[0.35]	[0.07]	[0.005]	
JCo3	0.53	0.29	0.14	0.04	0
(n = 4)	(0.32)	(0.42)	(0.21)	(0.05)	(0.004)
p = 0.18	[0.45]	[0.40]	[0.13]	[0.02]	[0.001]
JCo4	0.73	0.27	0		
(n = 2)	(0.56)	(0.38)	(0.06)		
p = 0.13	[0.76]	[0.23]	[0.02]		

[a] The data derived from Table 2.
[b] See Eq. [1] (Materials and Methods).
[c] Calculated frequency using Eq. [1] with p = 0.25 and assumptions described in the text.
[d] Average of experimental frequencies of alanine codon incorporation at targeted positions for single-oligo library calculated from values presented in Fig. 4.
[e] Calculated probability of multiple mutants occurence using the average of experimental frequencies of alanine replacement as p in Eq. [1].

obtaining a collection of large statistical samplings of mutations has important implications for the understanding of structure–function relationships in proteins.

(ii) Our approach also facilitates the modulation of the statistical distribution of multiple mutants either during the oligo synthesis or by recombining various libraries once the effect of given mutations at a limited number of positions is known. No prior knowledge of the impact of single or multiple changes on protein function is necessarily required. At a low level of mutations, the size of the libraries is large, increasing the screening effort. At a high level of mutations, however, the preponderance of multiple mutants might result in a larger number of nonfunctional proteins without providing information relative to critical amino acid positions. The total number of different possible mutation combinations for n targeted sites is 2^n. Equation [2] permits the evaluation of the minimum number of individual colonies to screen to achieve a high degree of certainty of including all possible combinations of substitutions encoded by a mutagenic oligo population. For example, if $p = 0.25$, $n = 4$ ($F_4 = 0.004$; Table 3) with an efficiency of mutagenesis of 50%, then the minimum number of individual colonies to be screened to obtain at least onefold coverage of the 16 possible mutation combinations with a 99% degree of certainty is 575 clones. However, as some mutant combinations are underrepresented, the size of the library must be increased accordingly.

(iii) The PCR-based colony-screening procedure allows in the absence of phenotypic selection (a) the determination of the mutagenesis efficiency, (b) the evaluation of the percentage of alanine codon incorporation at targeted positions, and (c) the discrimination of wild-type molecules and the identification of mutants. DNA sequencing is not required for all the clones selected from the screening of the minimum number of colonies, reducing time-consumming efforts in DNA sequencing analysis. Up to 100 clones containing four potential mutation sites could be fully characterized in a day. Combined with a phenotypic screen, the approach should be a powerful addition to the spectrum of mutagenesis methods.

ACKNOWLEDGMENTS

We thank Dr. D. Altschuh, Dr. M. H. V. Van Regenmortel, and Dr. D. Y. Thomas for constant encouragement and continuous support. We thank Dr. P. Dumas for helping us with statistical analysis. We also acknowledge Dr. E. Weiss, Dr. M. Whiteway, D. C. Tessier, and J. Labrecque for a critical reading of the manuscript and for suggestions. This work was supported by the Ministère de la Recherche et de l'Espace and the Office Franco-Québécois de la Jeunesse.

REFERENCES

1. Zoller, M. J. (1991) *Curr. Opin. Struct. Biol.* **1,** 605–610.
2. Smith, M. (1985) *Annu. Rev. Genet.* **19,** 423–462.
3. Cunningham, B. C., and Wells, J. A. (1989) *Science* **244,** 1081–1085.
4. Shortle, D., Stites, W. E., and Meeker, A. K. (1990) *Biochemistry* **29,** 8033–8041.
5. Horovitz, A., and Fersht, A. R. (1990) *J. Mol. Biol.* **214,** 613–617.
6. Wells, J. A. (1991) *Methods Enzymol.* **202,** 390–411.
7. Thukral, S. K., Morrison, M. L., and Young, E. T. (1991) *Proc. Natl. Acad. Sci. USA* **88,** 9188–9192.
8. Altschuh, D., Tessier, D. C., and Vernet, T. (1994) *Protein Eng.* **7,** 769–775.
9. Dembowski, N. J., and Kantrowitz, E. R. (1994) *Protein Eng.* **7,** 673–679.
10. Wells, J. A. (1990) *Biochemistry* **29,** 8509–8517.
11. Gregoret, L. M., and Sauer, R. (1993) *Proc. Natl. Acad. Sci. USA* **90,** 4246–4250.
12. Sandberg, W. S., and Terwilliger, T. C. (1993) *Proc. Natl. Acad. Sci. USA* **90,** 8367–8371.
13. Reidhaar-Olson, J. F., and Sauer, R. T. (1988) *Science* **241,** 53–57.
14. Hill, D. E., Oliphant, A. R., and Struhl, K. (1987) *Methods Enzymol.* **155,** 558–568.
15. Derbyshire, K. M., Salvo, J. J., and Grindley, N. D. F. (1986) *Gene* **46,** 145–152.
16. Sondek, J., and Shortle, D. (1992) *Proc. Natl. Acad. Sci. USA* **89,** 3581–3585.
17. Cormack, B. P., and Struhl, K. (1993) *Nature* **262,** 244–248.
18. Glaser, S. M., Yelton, D. E., and Huse, W. D. (1992) *J. Immunol.* **149,** 3903–3913.
19. Pakula, A. A., and Simon, M. I. (1992) *Proc. Natl. Acad. Sci. USA* **89,** 4144–4148.
20. Sambrook, J., Fritsch, E. F., and Maniatis, T. (1989) Molecular Cloning: A Laboratory Manual, 2nd ed., Cold Spring Harbor Laboratory Press, Cold Spring Harbor, NY.
21. Munro, S., and Pelham, H. B. R. (1986) *Cell* **46,** 291–300.
22. Hochuli, E., Bannwarth, W., Döbelich, H., Gentz, R., and Stuber, D. (1988) *Bio/Technology* **6,** 1321–1325.
23. Sanchez-Pescador, R., and Urdea, M. S. (1984) *DNA* **3,** 339–343.
24. Zoller, M. J., and Smith, M. (1982) *Nucleic Acids Res.* **10,** 6487–6500.
25. Kunkel, T. A. (1985) *Proc. Natl. Acad. Sci. USA* **82,** 488–492.
26. Vieira, J., and Messing, J. (1987) *Methods Enzymol.* **153,** 3–11.
27. Hanahan, D. (1983) *J. Mol. Biol.* **166,** 557–580.
28. Yanish-Perron, C., Vierra, J., and Messing, J. (1985) *Gene* **33,** 103–119.
29. Saiki, R. K., Sharf, S., Faloona, F., Mullis, K. B., Horn, G. T., Erlich, H. A., and Arnheim, N. (1985) *Science* **230,** 1350–1354.
30. Sanger, F., Nicklen, S., and Coulson, A. R. (1977) *Proc. Natl. Acad. Sci. USA* **74,** 5463–5467.
31. Zhang, S., Zubay, G., and Golman, E. (1991) *Gene* **105,** 61–72.
32. Better, M., Chang, C. P., Robinson, R. R., and Horwitz, A. H. (1988) *Science* **240,** 1041–1043.
33. Kabat, E. A., Wu, T. T., Reid-Miller, M., Perry, H. M., and Gottesman, K. S. (1991) Sequences of Proteins of Immunological Interest, 5th ed., Department of Health and Human Services, Bethesda, MD.

The X-ray structure of an anti-tumour antibody in complex with antigen

Philip D. Jeffrey[1,3], Jürgen Bajorath[2], ChiehYing Y. Chang[1], Dale Yelton[2], Ingegerd Hellström[2], Karl Erik Hellström[2] and Steven Sheriff[1]

The crystal structures of the murine BR96 Fab and its human chimera have been determined in complex with the nonoate methyl ester derivative of Lewis Y (nLe^y) at 2.8 Å and 2.5 Å resolution, respectively. BR96 binds the carbohydrate in a large pocket which is formed by residues of all CDR loops except L2. The binding of the carbohydrate is mediated predominantly by aromatic residues in BR96. Analysis of the structure suggests that BR96 is capable of recognizing a structure larger than the Le^y tetrasaccharide, providing a possible explanation for its high tumour selectivity. The structure provides a rationale for mutagenesis experiments that have resulted in BR96 CDR loop mutants with increased affinity for nLe^y and/or tumour cells.

[1]Bristol-Myers Squibb Pharmaceutical Research Institute, P.O. Box 4000,Princeton, New Jersey 08543-4000, USA.
[2]Bristol-Myers Squibb Pharmaceutical Research Institute, 3005 First Avenue, Seattle, Washington 98121, USA
[3]Current address: Box 576, Memorial Sloan-Kettering Cancer Center, 1275 York Avenue, New York, New York 10021, USA
Correspondence should be addressed to S.S.

The generation of 'magic bullet' reagents to specifically attack tumour cells has long been the subject of intense effort[1]. Therapeutics derived from the monoclonal antibody BR96 represent a potential landmark since they show great promise in the treatment of several human cancers in preclinical trials[2]. BR96 has been shown to recognize Lewis Y (Le^y)[3], which is expressed on the surface of a variety of tumour cells[4]. BR96 was raised against human breast carcinoma cells and recognizes a tumour-associated antigen expressed at high levels on many human breast, lung and colon carcinomas and only at low levels on some differentiated epithelial cells, predominantly from the gastrointestinal tract[3]. BR96 recognizes the Le^y tetrasaccharide[3], a carbohydrate detected on human tumours, often in the form of trifucosylated Le^y (ref. 4; Fig. 1). All Le^y-related oligosaccharides are conformationally restricted around the N-acetyl-D-glucosamine (Nag) due to substituents at positions 3 and 4 (Fig. 1). Much of the Le^y recognized by BR96 on tumours is associated with the LAMP-1 membrane glycoprotein[5]. Membrane bound BR96 is rapidly internalized into tumour cells[5,6]. Thus an immunoconjugate, consisting of BR96 and the anti-cancer drug doxorubicin, was generated to selectively target and kill tumour cells[7]. The BR96-doxorubicin conjugate has been shown to cure nude mice from xenografted human carcinomas of the lung, breast and colon[2], and is currently the subject of phase I clinical trials. The nonoate methyl ester derivative of Le^y (nLe^y) was used to screen M13 phage libraries of BR96 mutants[8], designed with the aid of a three-dimensional model of the antibody[9]. These studies have resulted in the identification of BR96 mutants with increased affinity for tumour cells. In addition, one mutant shows increased binding to nLe^y, but not to tumours[8].

BR96 is the first reported structure of an anti-tumour antibody in complex with antigen and, in addition, the first structure of a fragment of a murine IgG3. To explore the structural basis of the specific BR96–Le^y interactions and the mutagenesis results, the crystal structure of the BR96–nLe^y complex was determined. Crystals of the mBR96 (mouse IgG3, κ) Fab–nLe^y and cBR96 (chimeric human IgG1, κ) Fab'–nLe^y complexes with identical variable fragements (Fvs) were obtained by co-crystallization as described previously[10] (Fab' indicates antigen-binding fragments produced with pepsin rather than papain). The structures of the complexes were determined by molecular replacement using several Fab structures as search models. Details of the structure determinations and the refinement are given in Table 1. Fig. 2 shows the electron density of the bound nLe^y ligand in the binding site of cBR96. The independently refined structures of the mBR96 Fab–nLe^y and cBR96 Fab'–nLe^y complexes are similar. After least squares superposition of the BR96 Fv framework regions the root-mean-squared deviations are 0.83 Å for all CDR loop atoms and 0.61 Å for all nLe^y atoms. The details of the BR96–nLe^y interactions are essentially identical in both structures. The analysis will be focused on the cBR96–nLe^y complex at 2.5 Å resolution.

Antibody–carbohydrate interactions

BR96 binds nLe^y in a large, deep pocket which is approximately 12 Å wide (VH to VL distance) and 10 Å deep

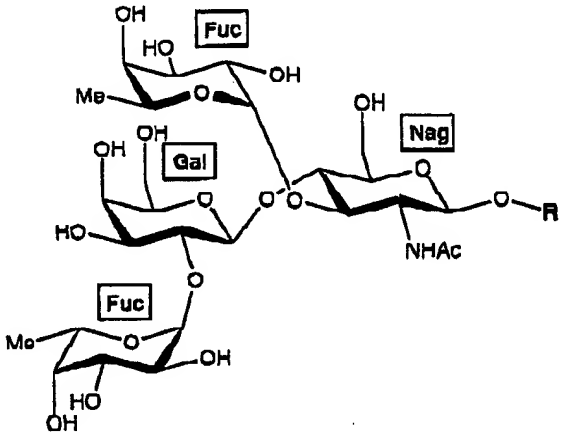

Nonoate methyl ester Lewis Y (nLe^y):

R = ——$(CH_2)_8COOCH_3$

Trifucosylated Lewis Y:

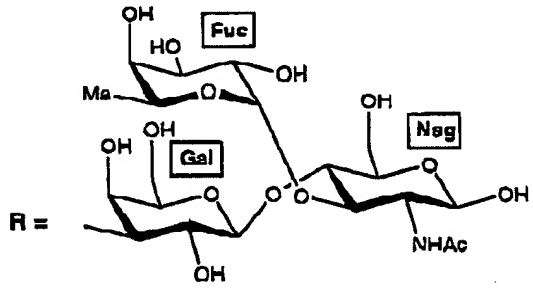

Fig. 1 Structures of the nonoate methyl ester Lewis Y (nLe^y) tetrasaccharide and trifucosylated Le^y. Le^y consists of four hexose units and is conformationally restricted around the Fuc4 (α1 → 3)Nag and Gal (β1 → 4)Nag glycosidic bonds. In trifucosylated Le^y (ref. 4) the Gal (β1 → 4) {Fuc (α1 → 3)} Nag unit is repeated, but is replaced by nonoate methyl ester in nLe^y.

(Fig. 3*a,c*). This pocket is predominantly formed by aromatic residues (5 Tyr, 1 Trp, 1 Phe and 1 His). The BR96 residues which contact nLe^y or which are at least partially buried[11,12] in the complex, and the contacts between BR96 residues and the individual nLe^y units (4 hexose units and the nonoate methyl ester group) are summarized in Tables 2 & 3, respectively. The binding of nLe^y buries 422 Å^2 of the BR96 surface. As has been observed in most other antibody–antigen complexes, the VH domain contributes the majority of the buried surface (79 %) and most of the contacts. More than half (55 %) of the buried surface on the antibody is contributed by the side chains of the aromatic residues (Table 2). These contacts to aromatic residues include hydrogen bonds from the side chains of two tyrosines and a tryptophan to Le^y (Fig. 3*b*). Other hydrogen bonds are formed by main chain atoms and by only one non-aromatic side chain, Gln H52A. All four hexose units of nLe^y are accommodated in the BR96 binding pocket (Fig. 3*a,c*): Fuc4 of nLe^y is deeply buried and is mainly involved in contacts to BR96 main-chain atoms (Table 3). The CDR H3 loop in BR96, with the exception of Trp H100A, contributes only main-chain atom van der Waals contacts and hydrogen bonds from five residues to the interaction with Le^y (Fig. 3*b*). In addition, the side chain of Asp H97 interacts with the nonoate methyl ester. The presence of all four hexose units of nLe^y is essential for binding; Le^x, which lacks Fuc1, does not bind to BR96 (ref. 3). Fuc1 interacts solely with residue His L27D of the long CDR L1 loop in BR96, however, the absence of Fuc1 would leave a part of the BR96 binding pocket unoccupied.

The intimate involvement of all four hexose units of nLe^y in binding to BR96 suggests high specificity of the interaction, but does not result in high affinity (~2 x 10^5 M^{-1} for Fab; ref. 8). This probably reflects the enthalpic penalty required to desolvate and the entropic penalty to immobilize the nLe^y ligand on binding. Energetic calculations suggest that much of the binding energy results from the hydrophobic effect due to burial of non-polar atoms (S. Sheriff & J. Novotny, personal communication using methods described in ref. 13). The non-carbohydrate nonoate methyl ester group of nLe^y interacts in an extensive manner with BR96. Of the 397 Å^2 of nLe^y surface, which is buried on binding to BR96, ~20 % is attributable to the nonoate methyl ester group. The pairwise residue interactions are listed in Table 3. This suggests that a carbohydrate extension (for example, → 3 Gal) at the O1 of the Le^y Nag unit could favourably contribute to the interaction with BR96. A Nag O1 carbohydrate extension (Fig. 1) would not affect the residual structure of the Le^y tetrasaccharide nor interfere with existing BR96–Le^y contacts. The structure suggests that BR96 can recognize carbohydrate antigens larger than the minimal Le^y tetrasaccharide, and that the relatively high tumour specificity[2,3] of BR96 may be the result of recognition of larger Le^y-related antigens found on tumour cells.

Other anti-Le^y antibodies have been reported[14,15] but their structures are unknown. The binding of all four hexose units of nLe^y inside a pocket represents a major difference of this structure in comparison with the only other antibody–carbohydrate complex structure known, Se155-4–Salmonella O-antigen complex[16–18]. In the Se155-4 structures only one hexose of the antigen is buried on complex formation whereas the others (from 2–6 hexoses) are located on the antibody surface. Kabat proposed many years ago that antibodies which recognize linear carbohydrate antigens display either groove- or cavity-shaped binding sites (reviewed in ref. 19). Neither Le^y nor Salmonella O-antigen are strictly linear carbohydrate chains, but the X-ray structures of Se155-4 and BR96 in complex with carbohydrate antigens are consistent with the proposed groove and cavity classes, respectively. Se155-4 has a pocket for abequose, but the carbohydrate binds along the surface of the antibody in such a way that many Se155-4 binding sites could attach to a long carbohydrate chain. In contrast, BR96 binds at the non-reducing end of the carbohydrate and thus represents a cavity-type antibody[19].

Table 1 Data collection and refinement statistics

Data Collection	mBR96 Fab–nLe^y	cBR96 Fab'–nLe^y
Space Group	$P2_12_12_1$	$P4_32_12$
a (Å)	69.4	81.7
b (Å)	84.9	81.7
c (Å)	86.8	166.3
Maximum Resolution (Å)	2.78	2.5
Observations (no.)	23962	59769
Unique Reflections (no.)	9937	20051
Completeness (%)	73.9	91.7
R_{merge} (%)[1]	7.0	5.9
$\langle I/\sigma_I \rangle$	12.6	5.1
Last Shell (Å)	2.95–2.78	2.75–2.51
Completeness (%)	43.8	90.8
$\langle I/\sigma_I \rangle$	3.8	3.6
Refinement		
Resolution range (Å)	8–2.78	8–2.5
Number of reflections ($\|F\| > 1\sigma F$)	8858	17177
Number of atoms	3427	3315
R-value	0.197	0.238
r.m.s.d. bond length (Å)	0.008	0.009
r.m.s.d. bond angle, °	1.6	1.6
r.m.s.d. dihedral angle, °	27.5	27.1
r.m.s.d. improper angle, °	1.4	1.3
Coordinate error (Å)	0.30	0.37

[1] $R_{merge} = \Sigma_i(\Sigma_j |I_{ij} - \langle I_i \rangle|)/\Sigma_i \langle I_i \rangle$; I_{ij} is the scaled intensity of the jth observation of each unique reflection i and $\langle I_i \rangle$ is the mean value.
[2] Method of Luzzati[27].

In other protein–carbohydrate complexes, carbohydrate ligands interact predominately with negatively charged, amide and aromatic side chains[20–22]. Aromatic groups stack with hexose rings, while the side chains of Asp, Asn, Glu and Gln form most of the hydrogen bonds to the carbohydrate[20,21]. In both the Se155-4 (ref. 16) and BR96 complexes, the interactions are qualitatively different. Most of the hydrogen bonds to the carbohydrate ligand are made with the aromatic side chains or with main chain atoms. Moreover, the aromatic groups are generally not stacked against the hexose rings. Rather, the preponderance of aromatic side chains in the antibody–carbohydrate interactions is consistent with the relatively high frequency of aromatic residues in antibody combining sites[25].

Higher affinity mutants

Saturation mutagenesis of BR96 CDR loop residues and selection in M13 phage expression libraries has resulted in the isolation of three mutants with higher affinity to either nLe^y or tumour cells. A triple mutant in CDR loop H1 (Thr 28 → Pro, Ser 30 → Ala, Asp 31 → Ser) showed an approximate fourfold increase in binding to nLe^y, but not to tumours. Two separate mutations in CDR loops H2 (Gly 53 → Asp) and H3 (Asp 97 → Ala) each increase the binding to tumour cells approximately fivefold. The H2 mutation, however, shows only marginal improvement with nLe^y, whereas the H3 mutation equally enhanced binding to both antigens[8].

Since none of the three changes in H1 affect a structural determinant position[24] of the canonical H1 loop in BR96 and since Thr H28 has acceptable ϕ,ψ angles for proline, a significant conformational change of H1 is not expected as a result of these mutations. In the BR96–nLe^y complex, however, the charged side chain of Asp H31 contacts the methylene moiety of the nonoate methyl ester group of nLe^y. This unfavorable interaction would be diminished as a consequence of the Asp → Ser mutation. This is likely to explain the better binding of the mutant to nLe^y. This change does not affect existing molecular contacts between BR96 and the Le^y tetrasaccharide. On tumour cells Asp H31 may interact with a carbohydrate extension providing an explanation for the differential effects on nLe^y and tumour cells.

CDR loop H2 adopts a canonical structure type 3 (ref. 24) in the BR96–nLe^y complex, which usually requires the presence of a Gly at position 54 in the loop due to

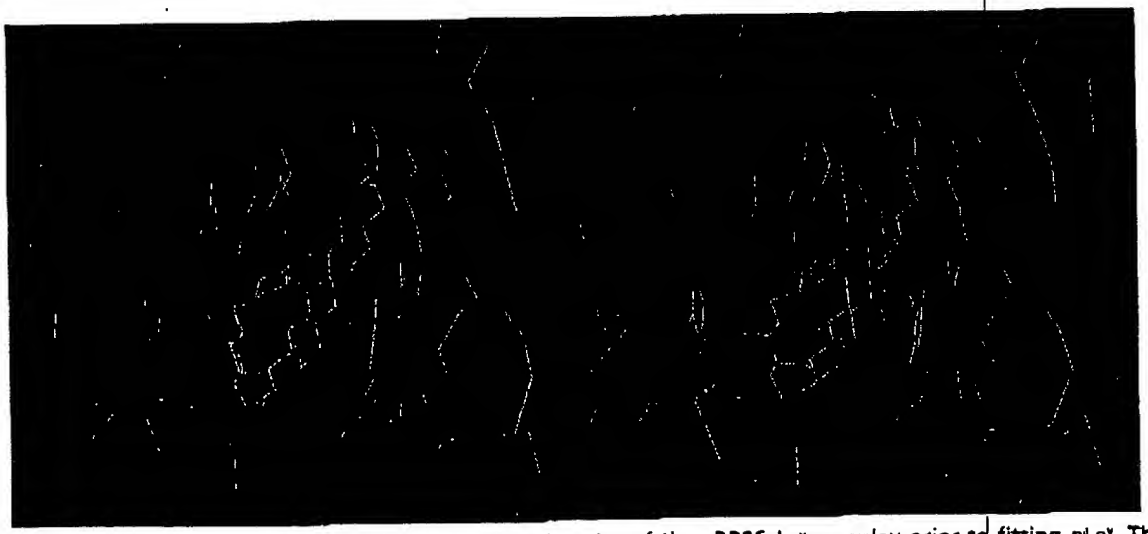

Fig. 2. Stereo diagram of $2|F_o|-|F_c|$ electron density in the binding site of the cBR96–Le^y complex prior to fitting nLe^y. The map was contoured at 1σ. The electron density is shown in dark blue, the final nLe^y model in yellow and BR96 in cyan. Map calculated by X-PLOR[28] and displayed in the program CHAIN[29].

unfavourable ϕ,ψ angles. Since BR96 contains glycines at position 53 and 54, the H2 loop may adopt more than one conformation[9]. However, in both structures these two glycines are in well-resolved electron density with carbonyl bulges and average or below average *B*-factors. The mutation Gly H53 → Asp should generally stabilize the H2 canonical motif in BR96 in the absence of antigen. Gly H53 is not a nLe^y contact residue, and model building suggests that the side chain of Asp at position 53 does not contact the nLe^y. That this mutation preferentially improves tumour-antigen binding provides further support for the hypothesis that BR96 binds a larger Le^y structure *in vivo*.

In contrast to the mutated residues in H1 and H2, Asp H97 interacts with both the tetrasaccharide and the

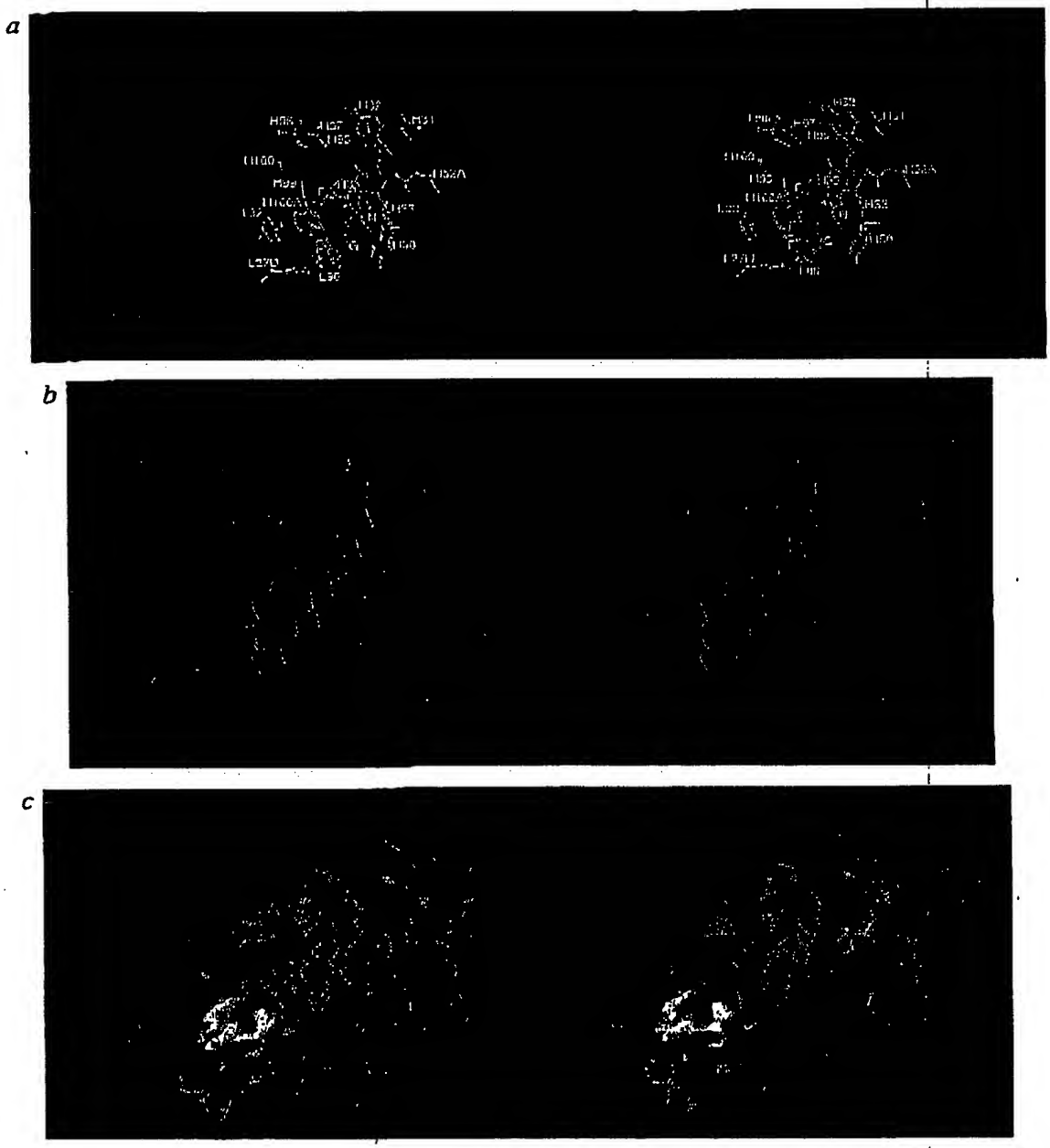

Fig. 3 Stereo views of Lewis Y binding to cBR96. *a*, nLe^y is shown in cyan, the side chains of contacting residues are shown in yellow. CDR loops are displayed in rose and framework regions in magenta. Figure produced with the program RIBBONS[28]. *b*, Hydrogen bonds between nLe^y (yellow) and BR96 (cyan) are shown in red. Figure produced with the program CHAIN[33]. *c*, The binding pocket of cBR96 with the model of Le^y bound. Protein surface is displayed in green (for convex surfaces) to dark gray (for concave surfaces) and the Le^y is shown in cyan. Figure produced with the program GRASP[40].

Table 2 Buried and contacting residues in mBR96–nLe^y and cBR96–nLe^y complexes

residue[1]	Partially Buried[2]		Contacting		Hydrogen bonds			
					mBR96		cBR96	
	mBR96	cBR96	mBR96	cBR96	atoms	Dist. Å	Atoms	Dist. Å
L 27D His	X	X	X	X	NE2-Gal O3	3.1	NE2-Gal O3	3.2
L 27E Asn	X	X						
L 32 Tyr	X	X	X	X				
L 94 Val	X	X						
L 96 Phe	X	X		X				
H 28 Thr	X	X						
H 31 Asp	X	X	X	X				
H 32 Tyr	X	X	X	X	OH-Non O10	3.1	OH-Non O1	2.9
H 33 Tyr	X	X	X	X	N-Nag O7	3.2	N-Nag O7	3.1
H 35 Tyr	X	X	X	X	OH-Fuc4 O3	2.7	OH-Fuc4 O3	2.5
					OH-Gal O6	2.7	OH-Gal O6	2.7
H 50 Tyr	X	X	X	X				
H 52A Gln	X	X	X	X	NE2-Nag O1	2.8	NE2-Nag O1	3.1
H 56 Ile	X	X						
H 95 Gly	X	X	X					
H 96 Leu	X	X	X	X				
H 97 Asp	X	X	X	X			OD1-Non O1	3.0[3]
H 99 Gly	X	X	X	X				
H 100 Ala	X	X	X	X	N-Fuc4 O4	3.3	N-Fuc4 O4	3.1
					O-Fuc4 O3	3.0	O-Fuc4 O3	2.9
							O-Fuc4 O4	3.2
H100A Trp	X	X	X	X			NE1-Gal O6	3.3

[1]Kabat numbering[38].
[2]Buried surface area determined by the program MS[12] with a 1.6 Å probe sphere and van der Waals radii from Gelin & Karplus[30]. Contacts were determined by the method of Sheriff[11]. As no uniform criteria for the assessment of 'contacts' exist, we use 'buried surface area' as an encompassing definition, which is less restrictive than 'contacts'. See Sheriff[11] for further explanation.
[3]Crystallographic model was refined in X-PLOR with electrostatics turned off. Moreover, the model does not contain potentially participating water molecules that could explain this apparently unfavourable interaction.

nonoate methyl ester. The main chain of this residue contacts Nag3 (Table 2) while the Asp H97 side chain, although partially solvent-exposed, contacts the nonoate methyl ester. The structural consequences of the Asp H97 → Ala mutation remain unclear, but the mutation may lead to enhanced van der Waals interactions between H3 and nLe^y. Furthermore, removal of a negative charge from the vicinity of the partial negative charge on the carbonyl oxygen on the N-acetyl group of Nag may be energetically favourable. To resolve how these mutations affect the BR96 interaction with tumour cells, it will be necessary to study both the complex of BR96 with a larger Le^y antigen and complexes of BR96 mutants.

Methods

Data collection and molecular replacement. Data were collected as previously described for both complexes[10]. Only one crystal of satisfactory size was obtained for mBR96 Fab–nLe^y complex and radiation decay limited the amount of data that could be collected (Table 1). For refinement of the cBR96 Fab'–nLe^y complex, data (Table 1) were collected with an R-axis IIc at Molecular Structure Corporation (The Woodlands, TX, USA).

The structures of the cBR96 Fab'–nLe^y and mBR96 Fab–nLe^y complexes were determined by molecular replacement. Approximately 15 Fab models were used in conjunction with MERLOT[25], BRUTE[26] and X-PLOR[27,28] to determine the structure of the cBR96Fab'–nLe^y complex. A rotation function solution was obtained with the Fv of 17/9 (1HIL; ref. 29). The Fvs of the other Fab models were superimposed on the rotated 17/9 Fv to create models with 17/9 Fv and the elbow bend and constant region of the Fab. The hybrid model of 17/9 Fv with the constant domains of 40–50 Fab, an anti-digoxin antibody[30], yielded the highest correlation coefficient at the filtering step. The results of the correlation coefficient translation function revealed the space group to be $P4_32_12$ as opposed to its enantiomorph. After obtaining the molecular replacement solution for the cBR96 Fab'–nLe^y complex, the VL domain was replaced with that of B13I2 (1IGF; ref. 31) and non-identical residues were trimmed to Ala or Gly and peptide segments in the CDRs were set to zero occupancy. The model was rebuilt, divided into Fv and CL:CH1 fragments[23], and used in conjunction with MERLOT[25], BRUTE[26] and X-PLOR[27,28] to determine the structure of the mBR96 Fab–nLe^y complex.

Refinement. Maps were calculated with X-PLOR[28] and models examined and manually rebuilt using CHAIN[33]. Refinement by simulated annealing was performed with X-PLOR[28] using the Engh and Huber[34] topology and parameter set, but with param19x.pro force constants (P.D.J., unpublished). At the end of refinement for both the mBR96Fab–nLe^y and cBR96Fab'–nLe^y complexes, the Engh and Huber topology and parameter sets distributed with X-PLOR (parhcsdx.pro and param3.cho for Le^y) were used. In both parameter sets the disulphide bond dihedral restraints were modified for the immunoglobulin disulphide bond, which has a χ_2 of −180° (ref. 35; P.D.J., unpublished). The relatively high *R*-value for the cBR96Fab'–nLe^y complex can be rationalized by the

Table 3 Lewis Y residues contacting BR96 residues

Le^y Residue	BR96 Residues[1]	
	Light chain	Heavy chain
Fuc 1	His 27D	
Gal 2	His 27D. Phe 96	Tyr 33, Tyr 35, Tyr 50, Trp 100A
Nag 3		*Asp 31*, Tyr 32, Tyr 33, Gln 52A, *Asp 97*
Fuc 4	Tyr 32	Tyr 35, *Gly 95, Leu 96, Gly 99, Ala 100*, Trp 100A
Nonoate Methyl Ester		Asp 31, Tyr 32, Gln 52A, Asp 97

Residues in italics interact through main chain only.

[1]Kabat numbering[38].

extremely high mobility of the CL:CH1 domain dimer (average B of 65 Å² versus 34 Å² for Fv), which is consistent with CL:CH1 not being involved in lattice contacts. In the cBR96Fab'–nLe^y complex, convincing electron density could not be found for residues L1–L2, L212–L214 (C terminus), H1 and H125–H135, which are typically poorly ordered in Fab structures.

After the CDR loops were built, residual electron density in the binding pocket was fitted with a model of Le^y. The Le^y tetrasaccharide was constructed using the BUILDER module of InsightII (Biosym Technologies, San Diego) and low energy conformers were generated. When the maps showed electron density attributable to the nonoate methyl ester group, it was added to the model in extended conformation using CHAIN[29]. Initially, the density in the binding pocket of the mBR96Fab–nLe^y complex could be fitted with a twofold ambiguity, with the positions of Gal 2 and Fuc 4, and those of Fuc 1 and Nag 3 interchangeable. The ambiguity was resolved when the cBR96Fab'–nLe^y complex was examined and showed clear density for the current interpretation. Moreover, the $2|F_o|-|F_c|$ electron density map of the cBR96Fab'–nLe^y complex showed the nonoate methyl ester group, which confirmed the position of Nag 3 (Fig. 2). Re-examination of the mBR96Fab–nLe^y complex also revealed corresponding electron density.

Structure analysis. Molecular surfaces were calculated by the method of Connolly[12] with a 1.6 Å probe sphere and van der Waals radii from Gelin & Karplus[36] so that the results might be directly compared with those in ref. 11. van der Waals contacts were calculated by the method of Sheriff[11]. Coordinates have been deposited in the Protein Data Bank with accession numbers 1CYL and 1CLZ with a hold of one year from publication.

Received 27 January; accepted 17 April 1995.

Acknowledgements
We thank T. Lavole, J. Novotny and J. Villafranca for encouragement and helpful discussions.

1. Hellström, K.E. & Hellström, I. Principles of tumour immunity: tumour antigens. In *Biologic Therapy of Cancer* (Eds, DeVita, V.T., Jr, Hellman, S., & Rosenberg, S.A.) 35–92. (J.B. Lippincott Co., Philadelphia; 1991).
2. Trail, P.A. *et al.* Cure of xenografted human carcinomas by BR96-doxorubicin immunoconjugates. *Science* **261**, 212–215 (1993).
3. Hellström, I., Garrigues, H.J., Garrigues, U. & Hellström, K.E. Highly tumour-reactive, internalizing, mouse monoclonal antibodies to Le^y-related cell surface antigens. *Cancer Res.* **50**, 2183–2190 (1990).
4. Hakomori, S. Aberrant glycosylation in tumours and tumour-associated carbohydrate antigens. *Advan. Cancer Res.* **52**, 257–331 (1989).
5. Garrigues, J., Anderson, J., Hellström, K.E., Hellström, I. Anti-tumour Mab BR96 blocks cell migration and binds to lysosomal membrane glycoprotein on cell surface microspikes and ruffled membranes. *J. cell. Biol.* **125**, 129–142 (1994).
6. Garrigues, J., Garrigues, U., Hellström, I., & Hellström, K. E. Le^y specific antibody with potent anti-tumour activity is internalized and degraded in lysosomes. *Am. J. Pathol.* **142**, 607–622 (1993).
7. Willner, D. *et al.* (6-Maleimidocaproyl)hydrazone of doxorubicin–a new derivative for the preparation of immunoconjugates of doxorubicin. *Bioconjugate Chem.* **4**, 521–527 (1993).
8. Yelton, D.E. *et al.* Affinity maturation of the BR96 anticarcinoma antibody *in vitro* by codon-based mutagenesis. *J. Immunol.* in the press.
9. Bajorath, J. Three-dimensional model of the BR96 monoclonal antibody variable fragment. *Bioconjugate Chem.* **5**, 213–219 (1994).
10. Cheng, C.Y., Jeffrey, P.D., Bajorath, J.Hellström, I., Hellström, K.E. & Sheriff, S. Crystallization and preliminary X-ray analysis of the monoclonal anti-tumour antibody BR96 and its complex with the Lewis Y determinant. *J. molec. Biol.* **235**, 372–376 (1994).
11. Sheriff, S. Some methods for examining the interactions between two molecules. *ImmunoMethods* **3**, 191–196 (1993).
12. Connolly, M.L. Analytical molecular surface calculation. *J. appl. Crystallogr.* **16**, 548–558 (1983).
13. Novotny, J., Bruccoleri, R.E. & Saul, F.A. On the attribution of binding energy in antigen—antibody complexes McPC 603, D1.3, and HyHEL-5. *Biochemistry* **28**, 4735–4749 (1989).
14. Pastan, I., Lovelace, E.T., Gallo, M.G., Rutherford, A.V., Magnani, J.L. & Willingham, M.C. Characterization of monoclonal antibodies B1 and B3 that react with mucinous adenocarcinomas. *Cancer Res.* **51**, 3781–3787 (1991).
15. Kaneko, T. *et al.* Preparation of mouse-human chimeric antibody to an embryonic carbohydrate antigen, Lewis Y. *J. Biochem, Tokyo* **113**, 114–117 (1993).
16. Cygler, M., Rose, D.R. & Bundle, D.R. Recognition of a cell-surface oligosaccharide of pathogenic Salmonella by an antibody Fab fragment. *Science* **253**, 442–445 (1991).
17. Bundle, D.R. *et al.* Molecular recognition of a Salmonella trisaccharide epitope by monoclonal antibody Se155-4. *Biochemistry* **33**, 5172-5182 (1994).
18. Bundle, D.R., Baumann, H., Brisson, J.-R., Gagné, S.M., Zdanov, A. & Cygler, M. Solution structure of a trisaccharide–antibody complex: comparison of NMR measurements with a crystal structure. *Biochemistry* **33**, 5183–5192 (1994).
19. Padlan, E. A. & Kabat, E. A. Modeling of antibody combining sites. *Meths Enzymol.* **203**, 3–21 (1991).
20. Quiocho, F.A. Carbohydrate-binding proteins: tertiary structures and protein-sugar interactions. *A. Rev. Biochem.* **55**, 287-315 (1986).
21. Vyas, N.K. Atomic features of protein-carbohydrate interactions. *Curr. Opin. Struct. Biol.* **1**, 732-740 (1991).
22. Bundle, D.R. & Young, N.M. Carbohydrate—protein interactions in antibodies and lectins. *Curr. Opin. struct. Biol.* **2**, 666–673 (1992).
23. Padlan, E.A. On the nature of antibody combining sites: unusual structural features that may confer on these site an enhanced capacity for binding ligands. *Proteins Struct. Funct. Genet.* **7**, 112–124 (1990).
24. Chothia, C. *et al.* The conformations of immunoglobulin hypervariable regions. *Nature* **342**, 877–883 (1989).
25. Fitzgerald, P.M.D. MERLOT, an integrated package of computer programs for the determination of crystal structures by molecular replacement. *J. appl. Crystallogr.* **21**, 273–278 (1988).
26. Fujinaga, M. & Read, R.J. Experiences with a new translation-function program. *J. appl. Crystallogr.* **20**, 517–521 (1987).
27. Brünger, A.T. Solution of a fab (26-10)/digoxin complex by generalized molecular replacement. *Acta crystallogr. A* **47**, 195–204 (1991).
28. Brünger, A.T. *X-PLOR version 3.1: A system for X-ray crystallography and NMR.* Yale University Press, New Haven (1992).
29. Rini, J.M., Schulze-Gahmen, U. & Wilson, I.A. Structural evidence for induced fit as a mechanism for antibody-antigen recognition. *Science* **255**, 959–965 (1992).
30. Jeffrey, P.D., Schildbach, J.F., Chang, C.Y., Kussie, P., Margolies, M.N. & Sheriff, S. Structure and specificity of the anti-digoxin antibody 40-50. *J. molec. Biol.*, **248**, 344–360 (1995).
31. Stanfield, R.L., Fieser, T.M., Lerner, R.A. & Wilson, I.A. Crystal structures of an antibody to a peptide and its complex with peptide antigen at 2.8 Å. *Science* **248**, 712–719 (1990).
32. Cygler, M. & Anderson, W.F. Application of the molecular replacement method to multidomain proteins. 1. determination of the orientation of an immunoglobulin Fab fragment. *Acta crystallogr.* **A44**, 38–45 (1988).
33. Sack, J.S. CHAIN — a crystallographic modeling program. *J. molec. Graph.* **6**, 224–225 (1988).
34. Engh, R.A. & Huber, R. Accurate bond and angle parameters for X-ray protein structure refinement. *Acta crystallogr. A* **47**, 392–400 (1991).
35. Richardson, J.S. The anatomy and taxonomy of protein structure. *Adv. prot. Chem.* **34**, 167–339 (1981).
36. Gelin, B.R. & Karplus, M. Side-chain torsional potentials: effect of dipeptide, protein and solvent environment. *Biochemistry* **18**, 1256–1268 (1979).
37. Luzzati, V. Traitement statistique des erreurs dans la determination des structures cristallines. *Acta crystallogr.* **5**, 802–810 (1952).
38. Kabat, E.A., Wu, T.T., Perry, H.M., Gottesman, K.S. & Foeller, C. Sequences of proteins of immunological interest (National Institutes of Health, Bethesda, MD) (1991).
39. Carson, M. Ribbons 2.0. *J. appl. Crystallogr.* **24**, 958–961 (1991).
40. Nicholls, A., Sharp, K.A. & Honig, B. Protein folding and association: insights from the interfacial and thermodynamic properties of hydrocarbons. *Proteins Struct. Funct. Genet.* **11**, 281–296 (1991).